Journal of Catalysis 276 (2010) 335–350

Contents lists available at ScienceDirect

Journal of Catalysis

journal homepage: www.elsevier.com/locate/jcat

The NO_x storage-reduction on $Pt—K/Al_2O_3$ Lean NO_x Trap catalyst

L. Castoldi [a], L. Lietti [a,*], P. Forzatti [a], S. Morandi [b], G. Ghiotti [b], F. Vindigni [b]

[a] Dipartimento di Energia, Laboratory of Catalysis and Catalytic Processes and NEMAS, Centre of Excellence, Politecnico di Milano, P.zza L. da Vinci 32, Milano, Italy
[b] Dipartimento di Chimica I.F.M. and NIS Centre of Excellence, Università di Torino, via P. Giuria 7, 10125 Torino, Italy

ARTICLE INFO

Article history:
Received 24 May 2010
Revised 17 September 2010
Accepted 25 September 2010
Available online 4 November 2010

Keywords:
$Pt—K/Al_2O_3$ catalyst
NO_x reduction mechanism
NSR catalysts
LNT systems
Temperature Programmed Surface Reaction
FT-IR spectroscopy.

ABSTRACT

The nature of stored NO_x and mechanistic aspects of the reduction of NO_x stored over a model $Pt—K/Al_2O_3$ catalyst sample are investigated in this paper, and a comparison with a model $Pt—Ba/Al_2O_3$ catalyst is also made.

It is found that at 350 °C on both the catalysts the storage proceeds with the initial formation of nitrites, followed by the oxidation of nitrites to nitrates. A parallel pathway involving the direct formation of nitrates species is also apparent; at saturation, only nitrates are present on the catalyst surface over both $Pt—K/Al_2O_3$ and $Pt—Ba/Al_2O_3$. However, whereas bidentate nitrates are present in remarkable amounts on $Pt—K/Al_2O_3$, along with ionic nitrates, only very small amounts of bidentate nitrates were observed on $Pt—Ba/Al_2O_3$.

Under nearly isothermal conditions, the reduction of the stored NO_x with H_2 occurs via an in series two-steps Pt-catalysed molecular process involving the formation of ammonia as an intermediate, like for the $Pt—Ba/Al_2O_3$ catalyst sample. However, higher N_2 selectivity is observed in the case of the $Pt—K/Al_2O_3$ catalyst due to the similar reactivity of the H_2 + nitrate and NH_3 + nitrate reactions. Accordingly ammonia, once formed, readily reacts with surface nitrates to give N_2, and this drives the selectivity of the reduction process to N_2. Notably, a strong inhibition of H_2 on the reactivity of NH_3 towards nitrates is also pointed out, due to a competition of H_2 and NH_3 for the activation at the Pt sites. Finally, the effect of water and CO_2 on the reduction process is also addressed. Water shows a slight promotion effect on the reduction of the nitrates by H_2, and no significant effect on the reduction by ammonia, whereas CO_2 has a strong inhibition effect due to poisoning of Pt by CO formed upon CO_2 hydrogenation.

1. Introduction

The transportation sector, and in particular diesel-equipped vehicles, represents a primary source of NO_x emissions. For this reason, regulations to control NO_x emissions are becoming very severe: in Europe, the next Euro 6 (2014) regulations require a drastic decrease of NO_x emission for diesel passenger cars, from the current 0.18 g/km set by Euro 5 down to 0.08 g/km.

Three Way Catalytic (TWC) converters currently used for stoichiometric gasoline engines are not effective in the reduction of NO_x for Diesel engines, which work under lean conditions. Viable solutions for the control of NO_x in this case are the urea-SCR technique, which accomplishes the NO_x reduction by injecting urea (a precursor of NH_3) in the exhaust gases, and the NO_x Storage Reduction (NSR) or Lean NO_x Trap (LNT) system [1–3].

Although the urea-SCR technology is preferred for heavy-duty vehicles and minivans, LNTs have been specifically developed for small engines [4]. The NSR technology, at first introduced by Toyota in the mid 90s [1], works in a cyclic manner [2]. Long lean phases, during which NO_x are stored on the catalyst, are alternated with short rich periods during which the exhaust is deliberately made rich to reduce the trapped NO_x to N_2, thereby regenerating the catalyst. For vehicle applications, the trapping or lean phase is typically 60–90 s long, while the regeneration or the rich phase is of the order of few seconds. NSR catalysts are composed of a high surface area support material (often γ-alumina or stabilized alumina), precious metals (usually a combination of Pt and Rh) and a basic component, such as Ba or K phases, which acts as NO_x storage material [5,6].

Several studies concentrated on the reactivity and characteristics of Ba-containing catalysts [7–13], but only few reports on the specific behaviour of K-based catalysts have been published in the literature. Toops and co-workers analysed by *in situ* DRIFT the NO_x storage on $Pt—K/Al_2O_3$ and the effect of H_2O and CO_2 on this step [14,15]. They concluded that NO_x is stored primarily in the form of ionic nitrates on the K component; nitrites are also observed at low temperatures (below 200 °C), for short adsorption times [16]. The nature of stored species (i.e. nitrites and nitrates) and the proposed adsorption mechanism parallel those already described in the case of $Pt—Ba/Al_2O_3$ catalysts [11,17].

* Corresponding author. Fax: +39 02 7063/8173.
E-mail address: luca.lietti@polimi.it (L. Lietti).

0021-9517/$ - see front matter © 2010 Elsevier Inc. All rights reserved.
doi:10.1016/j.jcat.2010.09.026

Investigations on the reduction of NO_x stored on K-containing catalysts are also rather scarce. On the other hand, in recent papers of various groups, mechanistic aspects of the reduction of NO_x stored over Ba-based NSR catalytic systems have been reported [18–21]. Some of us previously showed that the reduction of stored nitrates by hydrogen under nearly isothermal conditions does not involve the thermal decomposition of the adsorbed NO_x species as a preliminary step [22,23], but instead occurs via a low temperature Pt-catalysed route. In particular, it has been suggested that the regeneration of Ba-based NSR catalysts proceeds exclusively according to a two-steps in series molecular pathway in which the first step is the fast reaction of hydrogen with nitrates producing ammonia, followed by a slower reaction of NH_3 with nitrate species downstream to give N_2 [24–26]. The occurrence of such a two-steps in series pathway, along with the development of an H_2 front travelling in the reactor [24,27], is able to account for the temporal sequence of products obtained at the reactor exit during the regeneration of NSR systems, with nitrogen being initially produced with very high selectivity, followed by ammonia evolution.

The work here presented focuses on the analysis of the reduction steps when K replaces Ba as the storage component and hydrogen is used as a reductant. In particular, this study addresses the specific role of potassium in the reduction chemistry and specifically on the occurrence of (i) the Pt-catalysed route previously suggested for the reduction of stored NO_x in Ba-containing samples and (ii) the in series two-steps molecular pathway involved in N_2 formation [25]. For this purpose, the reduction with H_2 of NO_x stored over a model Pt—K/Al_2O_3 catalyst has been analysed by combined microflow transient reactivity experiments and FT-IR spectroscopy. Accordingly, NO_x have been adsorbed on the catalyst surface at 350 °C starting from NO/O_2; then the reactivity of the stored NO_x with H_2 has been investigated by means of Temperature Programmed Surface Reaction experiments (TPSR) and Isothermal Step Concentration experiments (ISC). The reduction has been carried out under nearly isothermal conditions with limited concentration of H_2 to prevent thermal decomposition of nitrates with release of NO_x in the gas phase during the lean-rich switch. The reduction of the stored NO_x with NH_3 has also been considered to clarify the potential role of this species as intermediate in N_2 formation.

In parallel with reactivity experiments, FT-IR spectroscopy was employed to obtain information about the nature, reactivity and evolution of surface species. Experiments have been accomplished in the presence and in the absence of water and of CO_2, to address the effect of these species on the reduction mechanism and on the reactivity of the stored NO_x. The results obtained over the Pt—K/Al_2O_3 catalyst sample in this study have been compared with those collected in the case of a correspondent Pt—Ba/Al_2O_3 catalyst [25] in order to highlight possible similarities and differences.

2. Experimental

2.1. Catalysts preparation and characterization

A homemade Pt—K/Al_2O_3 (1/5.4/100 w/w) catalyst has been used in this study. This sample has molar amount of K comparable to that contained in the Pt—Ba/Al_2O_3 (1/20/100 w/w) model catalyst previously used for similar studies [25] (0.146 mol K or Ba/100 g of Al_2O_3).

The catalytic system has been prepared by incipient wetness impregnation of a commercial alumina sample (Versal 250 from UOP) with aqueous solutions of dinitro-diammine platinum (Stream Chemicals, 5% Pt in ammonium hydroxide) and subsequently with a solution of potassium acetate (Aldrich, 99%). The powder has been dried at 80 °C and calcined in air at 500 °C for 5 h after each impregnation step [10]. The impregnation order (first Pt and then K) has been selected in order to ensure a good dispersion and stability of the noble metal and of the alkaline component on the alumina support, in line with recipes of Toyota patents [28].

The prepared catalyst sample has been characterized by XRD, HRTEM, surface area, pore size distribution and Pt dispersion measurements. XRD diffraction spectra have been recorded with a Philips PW 1050/70 diffractometer equipped with a vertical goniometer using a Ni-filtered Cu Kα radiation. HRTEM measurements were performed using a side entry Jeol JEM 3010 (300 kV) microscope. Surface area and pore size distribution have been determined by N_2 adsorption–desorption at 77 K with the BET method using a Micromeritics TriStar 3000 instrument. The Pt dispersion has been estimated by hydrogen chemisorption at 0 °C, upon reduction in H_2 at 300 °C, using a TPD/R/O 1100 Thermo Fischer Instrument.

2.2. Catalytic tests

Catalytic tests have been performed in a micro-reactor consisting of a quartz tube (7 mm I.D.), loaded with 60 mg of catalyst powder (70–100 μm). A total flow of 100 cm^3/min (at 1 atm and 0 °C) has been used in the experiments. The reactor was directly connected to a mass spectrometer (Thermostar 200, Pfeiffer), an UV-NO_x analyzer (LIMAS 11HW) and a micro-gas chromatograph for analysis of the reaction products [10,11,29].

Prior catalytic activity runs, the catalyst sample has been conditioned by performing few storage/regeneration cycles. For this purpose, NO_x have been adsorbed at 350 °C by imposing a rectangular step feed of NO (1000 ppm) in flowing He + 3% v/v O_2 until catalyst saturation. Then the NO and O_2 concentrations have been stepwise decreased to zero, followed by a He purge at the same temperature (350 °C). This leads to the desorption of weakly adsorbed NO_x species. After the He purge, catalyst regeneration (rich phase) has been carried out with H_2 (2000 ppm in He). Conditioning lasted until a reproducible behaviour was obtained; this typically required 3–4 adsorption/reduction cycles.

After catalyst conditioning at 350 °C, Temperature Programmed Surface Reaction (TPSR) and Isothermal Step Concentration (ISC) experiments have been performed.

(a) TPSR. In a typical TPSR experiment, after NO_x adsorption at 350 °C followed by a He purge at the same temperature, the catalyst has been cooled to room temperature (RT) under He flow. Then a rectangular step feed of H_2 (2000 ppm in He) or NH_3 (1000 ppm in He) has been admitted to the reactor at RT (H_2- and NH_3-TPSR, respectively) and the catalyst temperature has been linearly increased to 500 °C (heating rate 10 °C/min), while monitoring the concentration of the products exiting the reactor.
This procedure leads to a complete removal of the stored NO_x, as pointed out by the comparison of the amounts of NO_x adsorbed during the lean phase and the amounts of the N-containing species evolved during the TPSR run.

(b) ISC. In a typical Isothermal Step Concentration experiment (ISC), after NO_x adsorption at 350 °C, the reduction of the NO_x stored species has been carried out at selected temperatures, in the range 100–350 °C. Accordingly, after NO_x storage at 350 °C followed by a He purge at the same temperature, the catalyst temperature has been set at the desired value and a rectangular step feed of H_2 (2000 ppm in He) or NH_3 (1000 ppm in He) has been admitted to the reactor, thus leading to the reduction of the stored NO_x. At

the end of the regeneration procedure, the catalyst was heated up to 350 °C under He flow and eventually hydrogen was added to the reactor to complete the reduction of unreacted stored NO_x, if any. This procedure allowed the quantification of the residual NO_x species left after reduction at the various investigated temperature.

The role of water and of CO_2 in the reduction of the stored NO_x has also been addressed by performing the experiments in the presence of water vapour (1% v/v) and of both H_2O (1% v/v) and CO_2 (0.3% v/v). Unless otherwise specified, water or water and CO_2 were present during the regeneration phase only (i.e., not during the NO_x storage).

During the regeneration with H_2, N_2 and NH_3 have been observed as primary reduction products, along with minor amounts of NO. No N_2O has been observed. The reactor outlet products' concentration changes with time during the regeneration phase, and hence the selectivity also changes with time. Accordingly, the time-weighted average N_2 selectivity (S_{N2}) has been estimated, according to Eq. (a):

$$S_{N2} = \frac{2n_{N2}}{2n_{N2} + n_{NO} + n_{NH3}} \quad \text{(a)}$$

where n_{N2}, n_{NO} and n_{NH3} are the total molar amounts of N_2, NO and NH_3, respectively, evolved during the entire regeneration phase.

2.3. FT-IR analysis

Absorption/transmission IR spectra have been obtained on a Perkin-Elmer FT-IR System 2000 spectrophotometer equipped with a Hg-Cd-Te cryo-detector, working in the range of wavenumbers 7200–580 cm^{-1} at a resolution of 1 cm^{-1} (number of scans ~10). For IR analysis, powder catalyst has been compressed in self-supporting disc (of about 10 mg cm^{-2}) and placed in a commercial heatable stainless steel cell (Aabspec) allowing thermal treatments *in situ* under vacuum or controlled atmosphere. Pellet has been activated by heating in vacuum at 500 °C in order to remove carbonate surface species formed during the acetate decomposition. Besides, on catalyst left in the laboratory atmosphere for few months, the amount and thermal stability of the carbonates species slightly increase and a storage-reduction cycle, performed at 350 °C by admitting NO_2 and subsequently H_2, is necessary for their complete elimination [30]. Afterward, the catalyst has been oxidized in dry oxygen at 500 °C, and cooling in oxygen down to the selected temperature.

NO_x storage experiments have been performed by admitting freshly prepared NO/O_2 mixture (P_{NO} = 5 mbar; P_{O2} = 20 mbar) at 350 °C. IR spectra have been recorded at the same temperature at increasing exposure times. After the storage phase, the catalyst has been evacuated at 350 °C and cooled down to room temperature (RT). The interaction of H_2O (from RT up to 350 °C) or CO_2 (from RT up to 350 °C) or NH_3 (only at RT) with stored NO_x has been then carried out. Alternatively, after a storage phase, the catalyst has been evacuated at 350 °C and cooled down to 100 °C. The reduction of the stored NO_x has been then carried out by admitting dry H_2 (5 mbar) or wet H_2 (P_{H2} = 5 mbar; P_{H2O} = 10 mbar), and dry NH_3 (5 mbar) or wet NH_3 (P_{NH3} = 5 mbar; P_{H2O} = 10 mbar) at increasing temperature up to 350 °C. Moreover, the reduction of stored NO_x has been carried out by admitting dry H_2 along with CO_2 (P_{H2} = 5 mbar; P_{CO2} = 10 mbar) at increasing temperature up to 350 °C.

Further details on experimental apparatus and procedures can be found elsewhere [10,11,25,29].

3. Results and discussion

3.1. Catalyst characterization

The catalyst characterization has been already reported in a previous paper [30]. Here, we only recall some useful information. The specific surface area of the commercial alumina sample after calcination at 700 °C is near 200 m^2/g, while a slightly lower value has been measured for the Pt—K/Al_2O_3 sample (176 m^2/g). The surface area contraction was not accompanied by significant changes in the pore volume (0.96 cm^3/g for γ-Al_2O_3 and 0.90 cm^3/g for Pt—K/Al_2O_3). The pore radius is in the range 90–100 Å.

The XRD patterns of the pure alumina support (not shown) exhibit the reflections typical of microcrystalline γ-Al_2O_3 (JCPDS 10-425). In the XRD patterns of the calcined Pt—K/Al_2O_3 catalyst, the characteristic peaks of γ-Al_2O_3 have been detected; monoclinic K_2CO_3 (JCPDS 16-820) and cubic K_2O (JCPDS 23-493) phases have been hardly recognized, thus suggesting that the potassium phase is mainly amorphous and well dispersed. Also FT-IR spectra [30] revealed that carbonate species are present on the fresh Pt—K/Al_2O_3 sample; these species are almost completely removed by outgassing at 500 °C or after a storage-reduction cycle at 350 °C. Significant coverage of the alumina support by the K component is attained in the prepared sample, as confirmed by FT-IR analysis in the OH stretching region [30] that showed the disappearance of hydroxyl bands characteristic of the γ-Al_2O_3 surface outgassed at 500–550 °C and the appearance of a new weak band at 3716 cm^{-1}, reasonably assignable to hydroxyls on the K phase.

The Pt dispersion measured by H_2 chemisorption is near 65%. HRTEM images of calcined sample freshly prepared revealed that the Pt particle size distribution ranges between 0.7 and 2.5 nm (the mean size being d_{Pt} = 1.5 nm) and that the K phase is well dispersed on the alumina support [30].

3.2. ISC experiments at 350 °C and FT-IR analysis

In Fig. 1, the results obtained during a NO_x storage (Section A)-reduction (Section B) cycle carried out at 350 °C over the Pt—K/Al_2O_3 conditioned catalyst are presented. Fig. 1C and D shows, for comparison purposes, the results obtained under the same experimental conditions over the Pt—Ba/Al_2O_3 catalyst sample.

3.2.1. NO_x storage (Fig. 1A)

NO is admitted to the reactor at t = 0 s; after 20 s, the breakthrough of NO is observed, while the evolution of NO_2 is seen starting from 100 s. The outlet concentrations of both NO and NO_2 increase with time and tend to a stationary level, indicating that saturation of the catalyst surface with NO_x is almost attained. At the end of the storage, the NO_2 concentration is far from that corresponding to the equilibrium of the NO oxidation reaction to NO_2 in the presence of 3% v/v O_2 (NO_2 = 210 ppm vs. NO_{2eq} = 555 ppm at 350 °C).

Then, at 1200 s, the NO feed is switched off and a tail is observed in the NO and NO_2 concentration profiles, due to the desorption of weakly adsorbed NO_x species. An additional small NO desorption (not shown in the figure) is detected upon switching off the oxygen flow, as expected in view of the effect of the oxygen partial pressure on the stability of nitrate species, and in agreement with what observed in the case of Pt—Ba/Al_2O_3 catalyst [20].

The results obtained in the case of the storage carried out on the Pt—K/Al_2O_3 catalyst sample (Fig. 1A) are similar to those collected on the Pt—Ba/Al_2O_3 catalyst (Fig. 1C). During the storage phase, the NO_x concentration trace is similar although the PtBa catalyst shows a NO_x breakthrough higher than the PtK sample; besides the NO/NO_2 ratio is different. This could be ascribed to the different

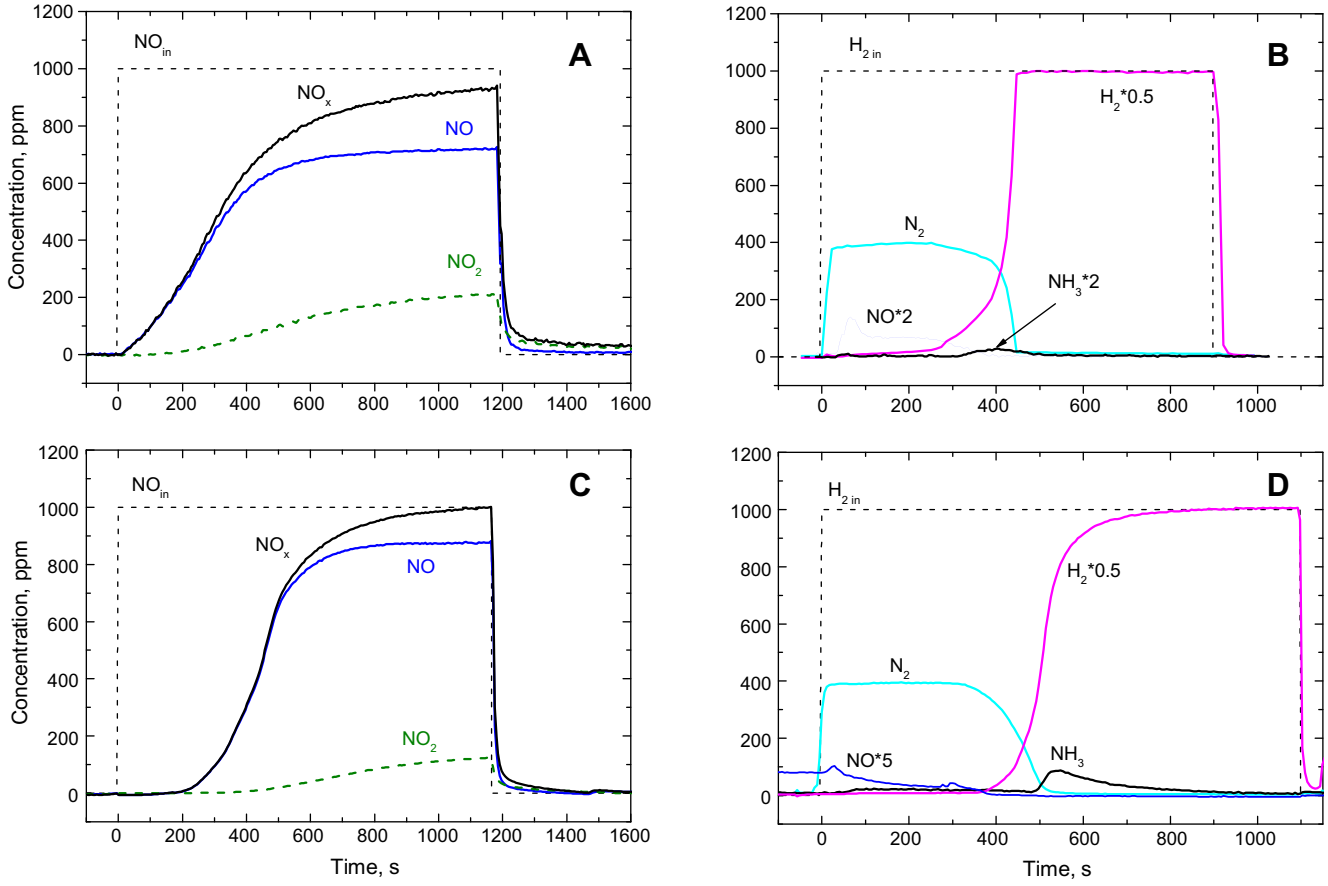

Fig. 1. Typical storage (A and C) and reduction (B and D) cycle at 350 °C over Pt—K/γ-Al_2O_3 (A and B) and Pt—Ba/γ-Al_2O_3 (C and D) catalysts (storage phase: NO 1000 ppm + O_2 3% v/v in He; reduction phase: H_2 2000 ppm in He).

reactivity of Pt in the NO oxidation, being its reactivity modified by the presence of storage components (K vs. Ba) having different electronic properties, in line with the results of FT-IR study showing very different surface properties of the noble metal [30,31].

The amounts of NO_x stored over the two catalytic systems are very similar, being near 5.1×10^{-4} and 5.9×10^{-4} mol NO_x/g_{cat} after He purge for the model Pt—K/Al_2O_3 and Pt—Ba/Al_2O_3 catalysts, respectively. Due to the similar molar loadings of the storage elements and the different stoichiometry of the K- and Ba-nitrates, the overall K and Ba utilization (i.e. the fraction of K and Ba sites involved in the storage of NO_x) is different, being close to 40% and 24% for K and Ba, respectively.

In situ FT-IR spectra of NO/O_2 interaction at 350 °C with the Pt—K/Al_2O_3 catalyst at increasing exposure times are reported in Fig. 2A: an initial formation of nitrite species is observed that rapidly evolve to nitrates. In particular, at low exposure times (10 s, curve a), both nitrites, of linear (ν_{N-O} mode, broad band at 1100–1000 cm^{-1}; $\nu_{N=O}$ mode at 1490 and 1536 cm^{-1}) and chelating ($\nu_{O-N-O,asym}$ mode at 1230 cm^{-1}) type, and ionic nitrates ($\nu_{NO3,asym}$ and $\nu_{NO3,sym}$ modes at 1370 and 1040 cm^{-1}, respectively) are present at the catalyst surface. At higher exposure times, the bands due to nitrite species decrease in intensity and eventually disappear after 2 min of exposure (curve e), simultaneously ionic nitrates increase and chelating bidentate nitrates ($\nu_{N=O}$, $\nu_{O-N-O,asym}$ and $\nu_{O-N-O,sym}$ modes at 1540, 1310 and 1010 cm^{-1}, respectively) appear and increase as well. After long exposure times (35 min, line g), corresponding to the surface saturation, only nitrates, both of the ionic and bidentate types, are present on the catalyst surface. Apart from the different ratio between the amounts of ionic and bidentate nitrates, they are the same species observed during the storage by Toops and co-worker [14] on a similar catalyst. It is worth of note that all the NO_x adsorbed species are related to the K phase, as previously reported [30], since the K phase completely covers alumina and NO_x species on the Al_2O_3 support are different from that formed on the Pt—K/Al_2O_3 catalyst.

Fig. 2B shows, for comparison purposes, the results obtained under the same experimental conditions over the Pt—Ba/Al_2O_3 catalyst, and already presented in previous papers (see for example Refs. [11,18]). On both Pt—K/Al_2O_3 and Pt—Ba/Al_2O_3 catalysts, nitrites species are formed at the beginning of the storage, being oxidized to nitrates in few minutes. Then only nitrates increase up to the saturation. These results indicate that on both the catalysts the storage proceed following the same pathways demonstrated for Pt—Ba/Al_2O_3 [11,32]. In particular, a pathway leads to the formation of nitrites which are then oxidized to nitrates

$$2NO + 0.5O_2 + O_s^{2-} \rightarrow 2NO_2^- \quad (1)$$

$$2NO_2^- + O_2 \rightarrow 2NO_3^- \quad (2)$$

and another one leads to the formation of NO_2, then stored following a dismutation process:

$$NO + 0.5O_2 \rightarrow NO_2 \quad (3)$$

$$3NO_2 + O_s^{2-} \rightarrow 2NO_3^- + NO \quad (4)$$

Actually, as mentioned above, these conclusions have been carefully demonstrated by comparison of FT-IR results obtained during NO/O_2 and NO_2 storage at 350 °C on both Pt—Ba/Al_2O_3 and Ba/Al_2O_3 samples [11,32]: briefly, during the NO_2 storage,

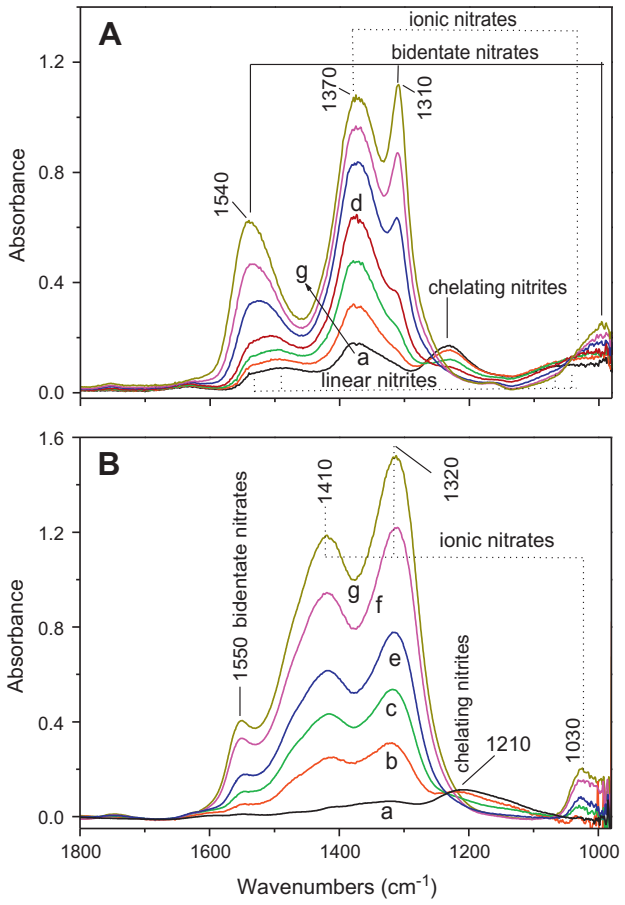

Fig. 2. Results of NO/O_2 adsorption FT-IR experiments over (A) Pt—K/Al_2O_3 and (B) Pt—Ba/Al_2O_3 catalysts. Spectra recorded after 10 s (curve a), 30 s (curve b), 1 min (curve c), 1 min 30 s (curve d), 2 min (curve e), 5 min (curve f) and 30 min (curve g) of exposure to NO/O_2 mixture (1:4, p_{NO} = 5 mbar) at 350 °C. Each spectrum is reported as difference from the spectrum run before NO/O_2 admission.

even at low contact times, only nitrate formation and no nitrites as stable intermediates were observed both in presence or in absence of Pt. For Pt—K/Al_2O_3 and K/Al_2O_3 catalysts, similar experiments performed in our laboratories lead to the same conclusions [33].

It is worth noting the different variety of NO_x surface species formed during the NO/O_2 storage on the two catalysts. On Pt—K/Al_2O_3 catalyst both chelating and linear nitrites are observed, differently from the case of Pt—Ba/Al_2O_3, where only chelating nitrites ($\nu_{O—N—O,asym}$ mode at 1210 cm^{-1}) were observed. Furthermore, at the saturation bidentate nitrates are present in remarkable amounts on Pt—K/Al_2O_3, while mainly nitrates of ionic type ($\nu_{NO3,asym}$ mode split at 1410 and 1320 cm^{-1}, and $\nu_{NO3,sym}$ mode at 1010 cm^{-1}) and minor amounts of bidentate nitrates ($\nu_{N=O}$ mode at 1550, the only visible one) were observed on Pt—Ba/Al_2O_3. In particular, in the following an evaluation of the relative amount of ionic and bidentate nitrates will be done. We will show that the two types of nitrates are coarsely present in comparable amounts on the surface over K-based catalyst (Fig. 2A).

3.2.2. Reduction phase

Fig. 1B shows the results obtained for the Pt—K/Al_2O_3 catalyst during the reduction carried out at 350 °C of the NO_x species stored at the same temperature. Upon H_2 addition to the reactor (t = 0 s), the stored NO_x are readily reduced to N_2. H_2 is completely consumed and the N_2 outlet concentration increases immediately to a level near 400 ppm. The N_2 concentration keeps almost constant for roughly 300 s and then decreases, in correspondence to H_2 breakthrough. The reaction is fast and is limited by the concentration of H_2; the overall consumption of 2000 ppm of H_2 and the formation of ca. 400 ppm N_2 well correspond to the stoichiometry of the reaction between nitrates and H_2:

$$2KNO_3 + 5H_2 \rightarrow N_2 + 2KOH + 4H_2O \quad (5)$$

The reduction of NO_x also produces water (not shown in the figure); accordingly, in reaction (5), the formation of KOH has been suggested due to the adsorption of water produced during the reduction, but the formation of K_2O cannot be excluded.

In addition to the nitrogen production, at the beginning of the reduction phase nonnegligible amounts of NO are also detected at the reactor outlet, possibly due to the desorption of NO_x adsorbed species and/or to the unselective reduction of the stored nitrates. Notably, no appreciable amounts of NH_3 and/or N_2O are observed at the reactor outlet.

At the end of the reduction step, the nitrates which have been stored during the previous adsorption cycle have been fully removed from the catalytic surface, as confirmed by the N-balance performed at the end of the cycle (the amounts of stored NO_x equal that of the N-containing species formed during the reduction phase). This observation is also in line with the FT-IR experiments showing the complete and fast removal of nitrates species stored onto the catalytic surface upon admission of hydrogen at 350 °C (not reported).

The reduction of NO_x stored over Ba-containing catalyst (Fig. 1D) shows slightly distinct features and occurs with formation of N_2 first and of an appreciable amount of NH_3 later on. Very small amounts of NO are also detected at the beginning of the reduction phase.

The following overall stoichiometries are hence involved in the reduction of the stored NO_x in the case of the Pt—Ba/Al_2O_3 catalyst:

$$Ba(NO_3)_2 + 5H_2 \rightarrow N_2 + Ba(OH)_2 + 4H_2O \quad (6)$$

$$Ba(NO_3)_2 + 8H_2 \rightarrow 2NH_3 + Ba(OH)_2 + 4H_2O \quad (7)$$

In particular, over the Pt—Ba/Al_2O_3 sample, the reduction of the stored NO_x is initially fully selective to N_2 (reaction (6)), whereas high selectivity to NH_3 is observed at the end of the reduction process (reaction (7)). The time-weighted average N_2 selectivity measured over the entire rich phase is however high, being near 93%.

The formation of both N_2 and NH_3 upon reduction of the stored NO_x over the Pt—Ba/Al_2O_3 model catalyst has been ascribed in previous studies to the occurrence of a two-steps in series molecular process [24–26]. Briefly, it has been suggested that H_2 readily reacts with nitrates to give ammonia (first step, reaction (7)), whereas in a second slower step the formed ammonia reacts with residual stored nitrates to give N_2:

$$3Ba(NO_3)_2 + 10NH_3 \rightarrow 8N_2 + 3Ba(OH)_2 + 12H_2O \quad (8)$$

Due to the fast reduction of stored nitrates by hydrogen to give ammonia and to the integral behaviour of the plug-flow reactor, an H_2 front develops which travels along the reactor [24–26]. Accordingly, NH_3 formed at the H_2 front according to reaction (7) reacts with NO_x stored downstream the front, leading to N_2 formation (reaction (8)). In line with our previous results [25] and with other literature reports as well [27,34], the occurrence of this pathway accounts for the observed temporal evolution of products during the reduction, with nearly complete nitrogen selectivity at the beginning of the rich phase followed by significant ammonia formation near the end of the regeneration stage (see Fig. 1D). This has also quantitatively accounted for by recent kinetic studies carried out under nearly isothermal conditions by some of us and by other groups as well [35,36].

Notably, in the case of the Pt—K/Al_2O_3 catalyst sample, a very small NH_3 formation is observed during the reduction of the stored NO_x (see Fig. 1B), as opposite to Pt—Ba/Al_2O_3. Accordingly, it is of interest to analyse the potential role of ammonia as intermediate in N_2 formation in the case of the Pt—K/Al_2O_3 catalyst sample as well. For this purpose, the reduction of the stored NO_x with H_2 and NH_3 has been performed by means of Temperature Programmed Surface Reaction (TPSR) experiments.

Moreover, as we want to study the effect of H_2O and CO_2 on the reduction process, the interaction of these molecules with the stored NO_x (i.e. with the bidentate and ionic nitrates present at the surface) has been preliminary examined by FT-IR spectroscopy, and results are given in the following paragraph.

3.3. Preliminary FT-IR study on the interactions of H_2O, CO_2 and NH_3 with the stored NO_x

Before starting the discussion, it is important to point out that the $\nu_{No3,asym}$ mode of free nitrate is double degenerate. The degeneration is maintained for the surface ionic species at high temperature. However, by decreasing the temperature to RT, the $\nu_{NO3,asym}$ mode splits into two bands at 1392 and 1368 cm^{-1}, showing a decrease in the symmetry of this adsorbed species (see curves a, both in Figs. 3A, B and 4A, B). This is reasonable, because a decrease of thermal energy decreases the mobility of the surface species.

In Fig. 3, the interaction of water (10 mbar) with the stored NO_x at increasing temperature is shown (nitrate region in Section A, and hydroxyl region in Section B). Curve a is the spectrum recorded at RT after the storage phase and evacuation at 350 °C. Notably, the evacuation causes the formation of small amount of chelating nitrites (mode at about 1270 cm^{-1}). Immediately after the H_2O admission at RT (curve b), the bands of bidentate nitrates ($\nu_{N=O}$ and $\nu_{O-N-O,asym}$ modes at 1548 and 1314 cm^{-1}, respectively) disappear and those of ionic nitrates ($\nu_{NO3,asym}$ mode split at 1392 and 1368 cm^{-1}) suddenly increase in intensity. The absorption related to the bending mode of the molecular adsorbed water is observed at about 1643 cm^{-1}, the associated stretching mode being the broad band centred at 3300 cm^{-1} in the OH stretching region (Fig. 3B). The rise of the temperature at 100 and 150 °C (curves c and d) causes a consistent desorption of molecular water (erosion of the bands at 1643 and 3300 cm^{-1}, Fig. 3B), but no significant changes in the NO_x region (Fig. 3A). Further temperature increase provokes the decrease of the ionic nitrate peaks, while those of bidentate ones starts to reappear (Fig. 3A, curves e–h) simultaneously with surface dehydration. The molecular water disappears at about 200 °C. However, at 350 °C, the surface is still markedly hydrated, showing an amount of OH bonded group bigger than in the case of the initial situation (compare curve a and h in Fig. 3B), and the modes of bidentate nitrates are only poorly reconstructed.

The experiments clearly demonstrate that the surface hydration transforms the bidentate nitrates in the ionic ones and is also confirmed by the isosbestic points visible in Fig. 3A.

The effect of ammonia is now considered. We have studied the adsorption of NH_3 at RT on the catalyst surface before and after the NO_x storage, being confident that no reduction by NH_3 was effective at RT and the results are reported in Fig. 4. When NH_3 (10 mbar) is adsorbed at RT before the NO_x storage (curve a'), the following observations can be done: (i) in the 1700–1000 cm^{-1} spectral region (Section A), the appearance of three bands at 1655 (weak), 1627 (weak), and 1110 cm^{-1} and (ii) in the 3800–2700 cm^{-1} spectral region (Section B), the appearance of an envelope of bands between 3400 and 3200 cm^{-1}. All these bands are assignable to the modes of adsorbed NH_3 polarized on the K^+ ions or bonded to the surface hydroxyls. In particular, the absorptions at

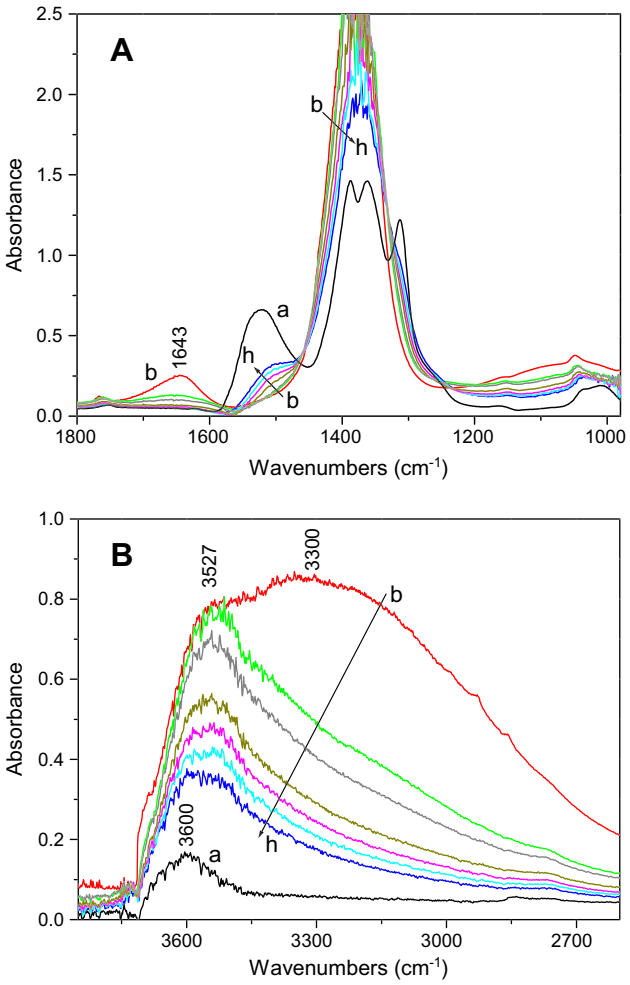

Fig. 3. FT-IR results on the changes induced by interaction, at different temperature, between H_2O and NO_x previously stored over the Pt—K/Al_2O_3 catalyst. (A) NO_x stretching region and (B) OH stretching region. Curves a, spectra of the NO_x stored by NO/O_2 at 350 °C, evacuated at 350 °C and cooled down to RT; curve b, after 10 min of exposure upon admission of H_2O (10 mbar) at RT; curve c–h, after 10 min of exposure at increasing temperature by step of 50 °C between 100 °C and 350 °C. Each spectrum is reported as difference from the spectrum run before NO/O_2 storage.

1655 and 1627 cm^{-1} are assignable to the δ_{asym} modes, the band at 1110 cm^{-1} to the δ_{sym} modes and the envelope between 3400 and 3200 cm^{-1} to the stretching modes. Curve (a) in Fig. 4 is the spectrum after the NO_x storage at 350 °C; when NH_3 (10 mbar) is adsorbed at RT after the NO_x storage (curve b), in the 1700–1000 cm^{-1} spectral region (Section A) a strong decrease of bidentate nitrate bands and a noticeable increase of those of ionic ones are observed simultaneously with an intensification and decrease in resolution of the $\delta_{asym}(NH_3)$ modes (only one broad peak is now present at 1627 cm^{-1}), a decrease in intensity of the $\delta_{sym}(NH_3)$ mode at 1110 cm^{-1}, and a decrease in the resolution of the $\nu_{asym}(NH_3)$ modes of adsorbed ammonia. Notably, the adsorption of ammonia strongly perturbs the stored nitrates, in a way very similar to the perturbation produced by water, i.e. transforming the bidentate nitrates in the ionic ones. It is also clear that in the presence of the stored NO_x the modes of adsorbed NH_3 are modified, indicating some changes due to its interaction with surface nitrates.

The effect of water and ammonia allows to evaluate the ratio between the amounts of bidentate and ionic nitrates at the end of a storage step. The calculation described in the following was

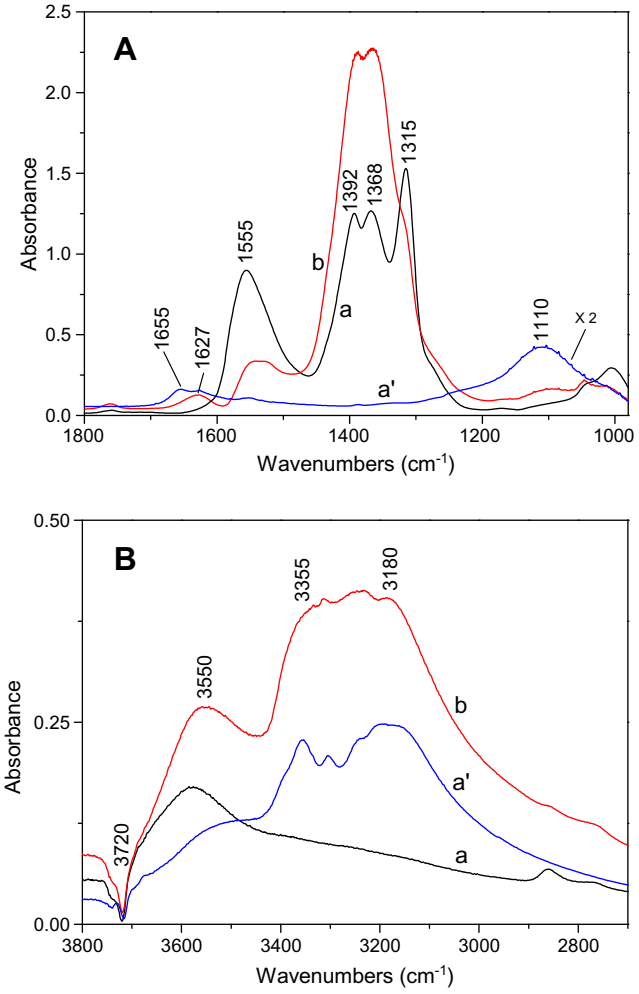

Fig. 4. FT-IR spectra obtained by interaction of NH_3 at RT with the Pt—K/Al_2O_3 catalyst: curves a', NH_3 admission before the NO_x storage (P_{NH3} = 10 mbar); curves b, NH_3 admission after the NO_x storage (P_{NH3} = 10 mbar). Curve a is the spectrum of the NO_x stored by NO/O_2 at 350 °C, evacuated at 350 °C and cooled down to RT. Each spectrum is reported as difference from the spectrum run before NO/O_2 storage. (A) Spectral region of NO_x stretching and NH_3 bending modes. (B) Spectral region of NH_3 stretching modes.

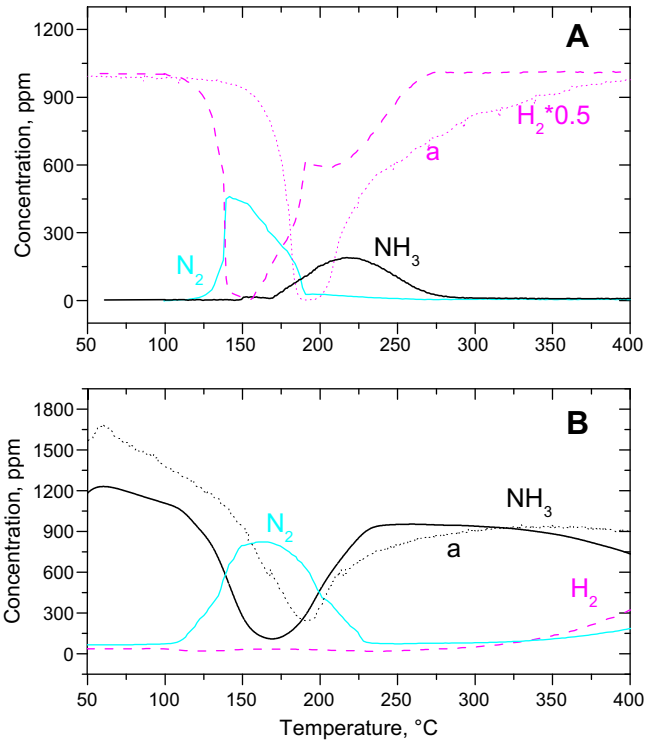

Fig. 5. (A) H_2-TPSR (2000 ppm in He); (B) NH_3-TPSR (1000 ppm in He) after NO/O_2 adsorption at 350 °C over the Pt—K/Al_2O_3 catalyst. Note: trace a in both the panels refers to H_2 or NH_3 concentration in the case of Pt—Ba/Al_2O_3 catalyst.

performed on the spectra shown for NH_3 interaction (Fig. 4A), since the spectra obtained for H_2O interaction are affected by noise in the ionic nitrate region, due to the thickness of the pellet. The integrated intensities of the bands at 1392 and 1368 cm^{-1} related to ionic nitrates before and after NH_3 interaction (I_{ion} and I_{ion}^{NH3}, respectively) were coarsely estimated. The ratio I_{ion}^{NH3}/I_{ion} is about 2. Taking into account that almost all bidentate nitrates are transformed into ionic ones, the value of the ratio $I_{ion}^{NH3}/I_{ion.}$ shows that the amounts of bidentate and ionic nitrates originally present on the surface are comparable.

Finally, the interaction of CO_2 at RT with the stored NO_x has been considered. No effects on the nitrates are observable in this case (spectra not reported). A minor amount of carbonates is formed on a small fraction of surface sites free from nitrates.

3.4. TPSR of stored NO_x with H_2 or NH_3 and FT-IR analysis

Fig. 5A shows the results obtained in the case of the H_2-TPSR experiment after NO_x adsorption at 350 °C. The H_2, N_2 and NH_3 concentration profiles are displayed as a function of temperature; the H_2 concentration profile measured in the case of TPSR experiments carried out for the Pt—Ba/Al_2O_3 catalyst [25] is also displayed for comparison purpose (trace ***a***, in the figure).

The H_2 profile has a complex shape: its concentration decreases starting from 110 °C, shows a minimum near 150 °C with full H_2 consumption and a second consumption peak with a minimum at 210 °C. H_2 consumption is accompanied by the evolution of N_2 and NH_3. N_2 is detected starting from 120 °C, its concentration at first grows slowly and then increases rapidly to the maximum value of 450 ppm. Then the N_2 concentration decreases and NH_3 production is observed, in correspondence with the second H_2 consumption peak centred at 210 °C.

During the reduction of the stored nitrates, water (not shown in the figure) is also formed. Neither NO nor N_2O has been detected in appreciable amounts during the run.

The data in Fig. 5A prove that nitrates stored at 350 °C can be reduced by H_2 already slightly above 100 °C, i.e. at temperatures well below those corresponding to their thermal decomposition (350 °C). In fact, a comparison with the results of TPD experiments where the stability of the nitrates stored at 350 °C over the Pt—K/Al_2O_3 sample has been investigated (results not reported for the sake of brevity) pointed out that in the absence of H_2 nitrates decompose only starting from the temperature of adsorption. Moreover, a comparison with the results of H_2-TPSR experiments carried out over a Pt-free sample (i.e. K/Al_2O_3) pointed out that the reduction of the stored nitrates is catalysed by Pt, since over K/Al_2O_3 the reduction is observed starting from the temperature of the thermal decomposition of the stored NO_x, i.e. 350 °C. This clearly indicates that over Pt—K/Al_2O_3 a Pt-catalysed route is responsible for the reduction of the stored nitrates, similarly to the case of Pt—Ba/Al_2O_3 [24,25].

The overall consumption of hydrogen observed during the TPSR run and the corresponding production of nitrogen and of ammonia are in line with the stoichiometries of reactions (5) and (9), respectively:

$$2KNO_3 + 5H_2 \rightarrow N_2 + 2KOH + 4H_2O \quad (5)$$

$$2KNO_3 + 8H_2 \rightarrow 2NH_3 + 2KOH + 4H_2O \quad (9)$$

In reactions (5) and (9), the formation of KOH is envisaged, due to the presence of water, although K_2O may also be present.

The presence of two H_2 consumption peaks in the TPSR trace may suggest the involvement of stored NO_x species having different reactivity. As a matter of fact, FT-IR data reported in the following show a different reactivity between ionic and bidentate nitrates. These H_2 consumption peaks are associated with the formation of different products, i.e. N_2 in the first peak and NH_3 in the shoulder at 210 °C.

Worth to note that calculations showed that the H_2 consumption observed in the low temperature range during the reduction in H_2 (i.e. below 130–140 °C of Fig. 5A) is slightly higher than that corresponding to N_2 production based on the stoichiometry of reaction (5). However, the overall H_2 consumption and the N_2 formation monitored during the TPSR run before NH_3 formation (i.e. below 170 °C) is in agreement with stoichiometry of the same reaction (5). This suggests that the reduction of the stored nitrates implies the formation of reduced intermediate adspecies whose formation involves the consumption of H_2 but not N_2 evolution. These partially reduced species might be tentatively associated with nitrites, formed from the stored nitrates at the beginning of the reduction process. This point will be discussed later on.

The comparison of the H_2 concentration trace with that obtained in the case of the Pt—Ba/Al_2O_3 catalyst sample (trace **a** in Fig. 5A) and discussed elsewhere [25] points out the greater reactivity of the K-containing sample in the reduction of the stored nitrates by H_2, since the H_2 consumption peak is observed in this case at lower temperature (110 °C vs. 145 °C).

Fig. 5B shows the results of a NH_3-TPSR experiment performed with NH_3 (1000 ppm in He), after NO_x adsorption at 350 °C. A complex shape in the NH_3 consumption is observed with desorption at low temperature and consumption at higher temperatures; the onset temperature of ammonia consumption (pointed out by N_2 formation) is observed near 105 °C and is very close to that detected for H_2. Then the NH_3 consumption proceeds quite rapidly, and the ammonia concentration shows a minimum of 100 ppm near 170 °C. Above 175 °C, the NH_3 concentration slowly increases and eventually decreases again above 300 °C.

Ammonia consumption is accompanied by N_2 formation in the range 105 °C–230 °C due to the reduction of the stored NO_x by NH_3, reaction (10):

$$6KNO_3 + 10NH_3 \rightarrow 8N_2 + 6KOH + 12H_2O \quad (10)$$

At higher temperature, above 300 °C, N_2 and H_2 evolution is observed due to the decomposition of ammonia to nitrogen and hydrogen according to the reaction:

$$2NH_3 \rightarrow N_2 + 3H_2 \quad (11)$$

During the reduction with ammonia, water (not showed in the figure) is also formed. Neither NO nor N_2O has been detected in appreciable amounts during the NH_3-TPSR experiment.

The comparison of the NH_3 consumption curves obtained over the Pt—K/Al_2O_3 and Pt—Ba/Al_2O_3 (curve **a**) samples clearly points out that the reactivity of NH_3 towards adsorbed nitrates is higher on the Pt—K/Al_2O_3 catalyst. In fact, over this catalyst, the minimum in the consumption of NH_3 is seen at much lower temperatures, in correspondence with the formation of N_2 (not shown in the case of the Pt—Ba/Al_2O_3 catalyst).

The reduction of the NO_x stored at 350 °C with H_2 and NH_3 has also been investigated by FT-IR spectroscopy (Fig. 6A and B). After the storage phase, the catalyst has been evacuated at 350 °C and cooled down to 100 °C (curves **a**), then FT-IR spectra were recorded

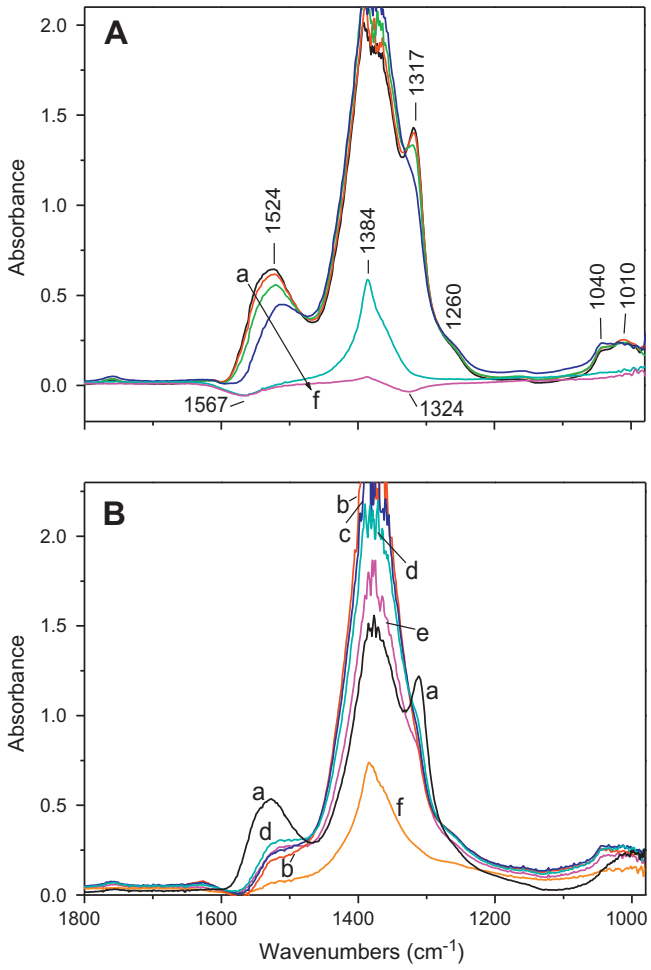

Fig. 6. FT-IR spectra recorded during the NO_x reduction over the Pt—K/Al_2O_3 catalyst at different temperatures. (A) Reduction in dry H_2 (P_{H2} = 5 mbar). Curve a, spectrum of the NO_x stored by NO/O_2 at 350 °C, evacuated at 350 °C and cooled down to 100 °C. Curves b–f, upon admission of dry H_2 at: 100 °C for 10 min (curve b), 120 °C for 10 min (curve c), 150 °C for 10 min (curve d), 200 °C for 10 min (curve e), 250 °C for 5 min (curve f). (B) Reduction in dry NH_3 (P_{NH3} = 5 mbar): curve a, spectrum of the NO_x stored by NO/O_2 at 350 °C, evacuated at 350 °C and cooled down to 100 °C. Curves b–f, upon admission of dry NH_3 at: 100 °C for 10 min (curve b), 150 °C for 10 min (coincident with curve b), 200 °C for 10 min (curve d), 250 °C for 10 min (curve e), 300 °C for 10 min (curve f). Each spectrum is reported as difference from the spectrum run before NO/O_2 storage.

upon the admission of H_2 or NH_3 at increasing temperatures, by steps of 20–50 °C, from 100 °C up to 350 °C, the exposure time at each temperature being 5–10 min.

In the case of H_2 (Fig. 6A), no sensible changes after exposure of 10 min at 100 °C are observed. Conversely, at 120 °C, the intensity of the bidentate nitrate peaks starts to decrease, the decrease being more marked after 10 min at 150 °C. However, at 150 °C, the bands related to ionic nitrates slightly increase in intensity; simultaneously, in the 3800–3000 cm^{-1} spectral region (not reported in the figure), a band related to OH stretching modes of surface hydroxyls appears. The temperature increase at 200 °C in dry H_2 provokes the complete reduction of bidentate nitrates and of the 90% of the ionic ones and, after 5 min at 250 °C, the reduction of nitrates is complete. These features can be easily explicated as follows: the bidentate nitrates initially present on the catalyst surface in absence of water begin to be reduced already at 120–150 °C, in accordance with the onset (110 °C) and the maximum (150 °C) of H_2 consumption observed in the TPSR experiment. However, at these temperatures, the water produced by their reduction is adsorbed in dissociative way at the surface, causing the transformation of a small fraction of them still present on the surface in

ionic nitrates, according with experiments illustrated in Fig. 3. Ionic nitrates become to be reduced only at 200 °C. These results put in evidence the different resistance to the reduction of the two types of surface nitrates, being the bidentate species the most reactive one, according to the two H_2 consumption peaks observed in the TPSR experiment.

FT-IR spectra obtained upon admission of dry NH_3 on stored NO_x are now considered (Fig. 6B). Immediately after the admission at 100 °C, the modes of bidentate nitrates markedly decrease while those of the ionic nitrates markedly increase and a weak band at 1628 cm^{-1} appears. Simultaneously, an envelope of bands at 3400–3200 cm^{-1} appears (not reported). No sensible changes after exposure of 10 min at 100 or 120 °C are observed. At 150 °C and 200 °C, it is possible to appreciate the decrease of the weak band at 1628 cm^{-1} and of those in the 3400–3200 cm^{-1} region, accompanied by an increase of bidentate nitrates and a decrease of the ionic ones. After 10 min at 250 °C, both bidentate and ionic nitrate peaks are reduced. A further increase of temperature to 300 °C enhances the reduction that is completed at higher temperatures.

The FT-IR results obtained during the reduction of stored NO_x with dry NH_3 can be explained as follows: (i) at 100 °C, the effect of the ammonia already described for the interaction at RT (see Fig. 4) is observed; (ii) the increase of the temperature up to 200 °C mainly provokes the ammonia desorption; and (iii) the reduction starts at 200 °C and is appreciable at 250 °C. As previously discussed, the presence of ammonia strongly perturbs the stored nitrates and these species modify the modes of adsorbed NH_3; in this condition, it could be difficult to evaluate the exact onset temperature of the reduction. Furthermore, differently from the reduction in hydrogen, in the case of ammonia both bidentate and ionic nitrates start to be reduced together, showing comparable reactivity on increasing the temperature. This result is in agreement with the shape of ammonia consumption in the TPSR experiment that does not show the shoulder observed for H_2-TPSR.

3.5. TPSR of stored NO_x with H_2 or NH_3 in the presence of water and FT-IR analysis

Fig. 7A shows the results obtained in the case of the wet H_2-TPSR experiment carried out after NO_x adsorption at 350 °C in dry conditions; the H_2 concentration profile obtained in the case of a TPSR experiment carried out over the Pt—Ba/Al_2O_3 catalyst [25] is also displayed for comparison purpose (trace **a** in the figure).

The concentration of H_2 decreases starting from 80 °C, at first slowly and then very rapidly so that the consumption is almost complete in the temperature range 140–170 °C. Then a shoulder with a minimum near 220 °C is also observed; eventually, the H_2 concentration increases to the inlet value of 2000 ppm. H_2 consumption is accompanied by the evolution of NH_3 and of N_2 at first, of N_2 only later on and finally of NH_3 only again at high temperature. The evolution of these products is observed starting from 110 °C, i.e. at temperatures slightly higher than that of H_2 consumption. The NH_3 concentration profile is rather complex, showing a peak near 140 °C and a second maximum near 210 °C, this last corresponding to the shoulder observed in the H_2 concentration profile. On the other hand, N_2 evolution shows an initial slow increase, near 120 °C, followed by a sharp increase near 140 °C, when the H_2 consumption is complete. The sharp increase in the N_2 formation corresponds to the sudden decrease in the NH_3 concentration: as will be discussed in the following, this suggests that the two-steps in series process for N_2 formation invoked in the case of the Pt—Ba/Al_2O_3 catalyst, involving ammonia as intermediate, is operating in the case of the Pt—K/Al_2O_3 sample as well.

Finally, during the reduction of the stored nitrates, water (not shown in the figure) is also formed, in addition to that already present in the feed stream. Neither NO nor N_2O has been detected in appreciable amounts.

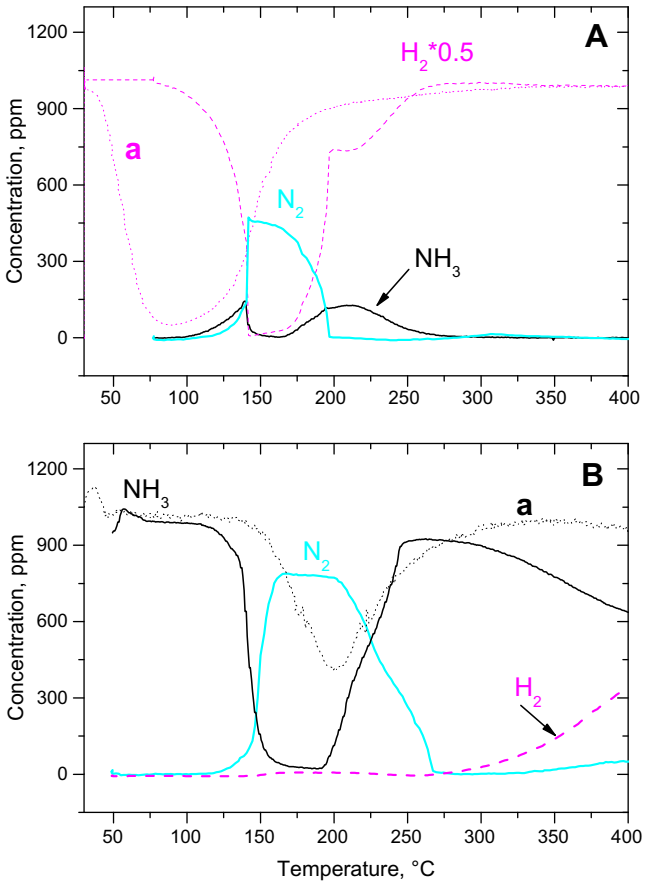

Fig. 7. (A) H_2-TPSR (2000 ppm + 1% v/v H_2O in He); (B) NH_3-TPSR (1000 ppm + 1% v/v H_2O in He) after NO/O_2 adsorption at 350 °C over the Pt—K/Al_2O_3 catalyst. Note: trace a in both the panels refers to H_2 or NH_3 concentration in the case of Pt—Ba/Al_2O_3 catalyst.

The comparison of the H_2 concentration trace with that obtained in the case of the Pt—Ba/Al_2O_3 catalyst sample (trace **a** in Fig. 7A) points out the greater reactivity of the Ba-containing sample in the reduction of the stored nitrates by H_2, since the threshold for H_2 consumption is observed in this case at lower temperatures (below 50 °C vs. 80 °C), as opposite to what observed in the absence of water.

Comparing Fig. 5A (dry H_2-TPSR) with Fig. 7A (wet H_2-TPSR), it appears that in the case of the Pt—K/Al_2O_3 catalyst sample water slightly favours the reduction of the stored nitrates by H_2, since in the presence of water the reaction is observed at slightly lower temperatures (80–100 °C vs. 110 °C). However, the presence of water does not apparently affect the high-temperature H_2 consumption, corresponding to the shoulder near 210 °C. The reason for which water slightly favours the reduction of the stored nitrates by H_2 has not been clarified so far. As already discussed elsewhere [25], a suggested pathway for nitrate reduction by H_2 involves the activation of the H_2 molecule over Pt, followed by H spillover towards nitrates. In this respect, it has been suggested that water increases the rate of reduction by favouring hydrogen spillover [25,37]. A significant enhancement is expected in this case in the reduction of nitrates stored far away from Pt sites, whose reaction implies the mobility of H adspecies on the surface. Specific effects of water on the mobility of adsorbed nitrates, a factor which may play a role in the reaction, can be also suggested, although this has been apparently ruled out by a recent study of Epling and co-workers [37] based on the results obtained upon

reduction of crystalline $Ba(NO_3)_2$ doped with Pt. We note however that in the case of our catalysts, water provokes significant changes in the nature of the adsorbed nitrates, already at RT, being bidentate nitrates transformed into ionic species. These aspects are presently under investigation in our laboratories.

The results obtained in the reduction with NH_3 in the presence of water of the nitrates stored at 350 °C (wet NH_3-TPSR) are shown in Fig. 7B. The H_2, N_2 and NH_3 concentration profiles are displayed as a function of temperature, along with the NH_3 concentration profile (trace **a**) obtained in a similar experiment carried out over the Pt—Ba/Al_2O_3 sample. The onset for ammonia consumption is observed in this case near 110 °C. Then the consumption of NH_3 proceeds quite rapidly and is almost complete near 170 °C. Above 190 °C, the NH_3 concentration slowly increases, shows a shoulder and eventually decreases again above 250 °C. Worth to note that, as in the case of the NH_3-TPSR carried out in dry conditions, during the wet NH_3-TPSR only N_2 has been observed among the reaction products, along with water (not showed in the figure), since neither NO nor N_2O has been detected in appreciable amounts.

The NH_3 consumption peak observed below 250 °C is accompanied by N_2 evolution, in line with the stoichiometry of reaction (10) already reported. At higher temperatures, above 300 °C, decomposition of ammonia according to the reaction (11) is observed. The comparison with the dry NH_3-TPSR experiments (Fig. 5B) points out that NH_3 is only slightly inhibited by the presence of water, as opposite to H_2. Indeed, under dry conditions, N_2 formation from NH_3 is observed near 105 °C, whereas in the presence of H_2O it is detected starting from 110 °C.

FT-IR spectra recorded in wet H_2 and in wet NH_3 at increasing temperature after NO_x adsorption at 350 °C are reported in Fig. 8A and B, respectively. After the storage phase, the catalyst has been evacuated at 350 °C and cooled down to 100 °C (curves **a**). In the case of the reduction in wet H_2 (Fig. 8A), immediately after wet H_2 admission (curve b), the effect of the hydration is observed: the modes of bidentate nitrates disappear while those of the ionic nitrates markedly increase, and a weak band at 1648 cm^{-1} appears. No sensible changes after exposure of 10 min at 100 °C are observed. After 10 min at 150 °C (curve **c**), the only change clearly appreciable is the decrease of the weak band at 1648 cm^{-1}, while after 10 min at 200 °C (curve **d**) this band disappears and ionic nitrate peaks are markedly reduced. A further increase of temperature to 250 °C (curve **e**) enhances the reduction that is only completed at higher temperatures. Due to the effect of water, it is difficult to evaluate at which temperature the reduction starts: in fact, between 150 and 200 °C surface dehydration is observed and bidentate nitrates should be reformed in small amount (see Fig. 3). However, in the presence of hydrogen, bidentate nitrates are immediately reduced and never observed in Fig. 8A after H_2/H_2O admission. Nevertheless, this experiment confirms that, also in presence of water, ionic nitrates are markedly reduced only at 200 °C.

When the reduction of the stored NO_x is carried out in wet NH_3 (Fig. 8B), the admission of the NH_3/H_2O mixture immediately provokes the disappearance of the bidentate nitrate absorptions and the increase of those of the ionic ones. No sensible changes are observed after 10 min of exposure at 100 °C or 150 °C. After 10 min of exposure at 200 °C, the intensity of ionic nitrates is reduced (curve **d**) but, differently than for the wet H_2, the modes of bidentate nitrates appear, indicating that the intensity decrease of the ionic nitrates can be due in part to their conversion into the bidentate ones; a further increase of temperature at 250 °C leaves the surface situation almost unaltered (curve e). Finally, at 300 °C, the reduction of both bidentate and ionic nitrates by NH_3 is well evident (curves f-h for increasing time), but it is rather slow and it will be completed only at 350 °C.

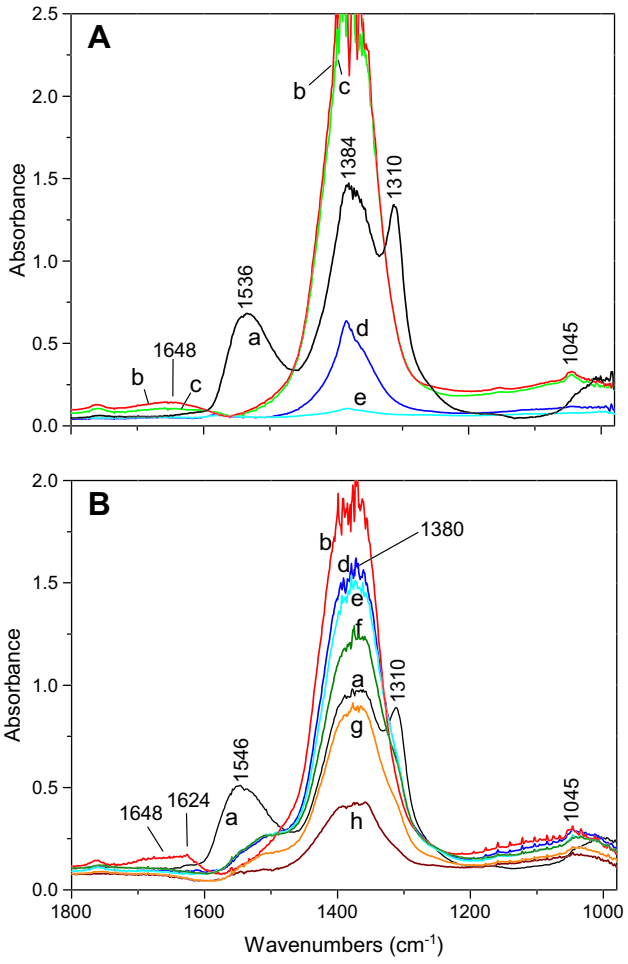

Fig. 8. FT-IR spectra recorded during the NO_x reduction over the Pt—K/Al_2O_3 catalyst at different temperatures. (A) Reduction in wet H_2 (P_{H2} = 5 mbar, P_{H2O} = 10 mbar) and (B) in wet NH_3 (P_{NH3} = 5 mbar, P_{H2O} = 10 mbar). Curves a, spectra of the NO_x stored by NO/O_2 at 350 °C, evacuated at 350 °C and cooled down to 100 °C. Curves b–h, spectra recorded upon admission of reducing mixtures at: 100 °C for 10 min (curve b), 150 °C for 10 min (curve c), 200 °C for 10 min (curve d), 250 °C for 10 min (curve e), 300 °C for 5 min (curve f), 300 °C for 10 min (curve g), 300 °C for 30 min (curve h). Each spectrum is reported as difference from the spectrum run before NO/O_2 storage.

Upon comparing Figs. 6A and 8A, it appears that in absence of water, H_2 begins to reduce bidentate nitrates at 150 °C, while both in wet or dry H_2 the reduction of ionic nitrates (the only present in wet conditions) begins at 200 °C. As mentioned above, due to the effect of water on the stored nitrates (see Fig. 3), in the case of wet H_2, it is difficult to evaluate at which temperature the reduction starts. Nevertheless, from the experiments in dry and wet conditions, it is clear that bidentate and ionic nitrates show a different reactivity, the bidentate being the more reactive ones. Note that in the absence of water at 250 °C also the residual surface carbonates are removed (negative bands at 1567 cm^{-1} and 1324 cm^{-1}, observed after reduction at 250 °C in Fig. 6A). This feature was not observed in the reduction in presence of water (see Fig. 8A).

On the other hand, in the reduction with ammonia, it is not well clear what happens in the presence of water under 300 °C (Fig. 8B), i.e. if the decrease of the bands of ionic nitrates is due to the dehydration and/or to the ammonia desorption, or to reduction. Indubitably, the reduction is effective at 300 °C but is rather slow. Conversely, in absence of water (Fig. 6B), the reduction begins at 250 °C, even at very slow rate, and is markedly increased at 300 °C at rate higher than in presence of water. This is in line with

the effect of water (slight inhibition) pointed out by NH_3-TPSR runs.

3.6. TPSR of stored NO_x with H_2/NH_3 mixtures in the presence of water

In order to further investigate the reactivity of H_2 and NH_3 with NO_x stored over the K-containing catalyst, TPSR experiment has been carried out by co-feeding H_2/NH_3 mixtures in the presence of 1% v/v H_2O (H_2/NH_3-TPSR), and results are presented in Fig. 9A.

In the co-presence of H_2 and NH_3, H_2 is consumed above 80 °C, i.e. at a temperature that is similar to that observed in the case of the wet H_2-TPSR previously discussed (Fig. 7A), and is accompanied by NH_3 formation due to the occurrence of reaction (9). The rate of H_2 consumption (and of the corresponding NH_3 production) is initially very slow; then, a sharp consumption peak is observed centred at 170 °C, accompanied by NH_3 consumption as well and by N_2 formation. A second broad H_2 consumption peak is observed at higher temperatures (above 200 °C), accompanied by ammonia production. This broad H_2 consumption peak well corresponds to the H_2 consumption peak observed near 210 °C in the wet H_2-TPSR run previously discussed (Fig. 7A). On the other hand, NH_3 is consumed at temperatures well above those measured during the NH_3-TPSR.

The co-presence of NH_3 and H_2 significantly affects the features of N_2 formation with respect to the experiments in which H_2 and NH_3 were separately fed to the reactor (compare Fig. 9A with Fig. 7A and B). First of all, during the H_2/NH_3-TPSR, the N_2 production is observed near 160 °C, i.e. at much higher temperatures if compared to both the H_2- and NH_3-TPSR experiments. In particular during the H_2/NH_3-TPSR experiment, the reactivity of ammonia with nitrates is inhibited by the presence of H_2 in the gas stream, while the reactivity of H_2 is not or only weakly affected by the presence of NH_3. Second, it is well apparent in the H_2/NH_3-TPSR (Fig. 9A) that ammonia reacts with adsorbed NO_x only in a strict temperature range (160–180 °C), i.e. when the H_2 concentration at the reactor outlet is null. This is a much higher temperature range if compared to the threshold observed for the NH_3 + nitrate reaction during the NH_3-TPSR experiments (110 °C, Fig. 7B). Since it has been previously clarified that the reaction of ammonia with stored nitrates leading to N_2 is catalysed by Pt [25], it is speculated that H_2 competes with ammonia for adsorption and activation on the Pt active sites, thus inhibiting NH_3 reactivity. Third, N_2 formation is observed during the H_2/NH_3-TPSR concomitantly with NH_3 consumption: this clearly indicates that NH_3 is involved in N_2 formation.

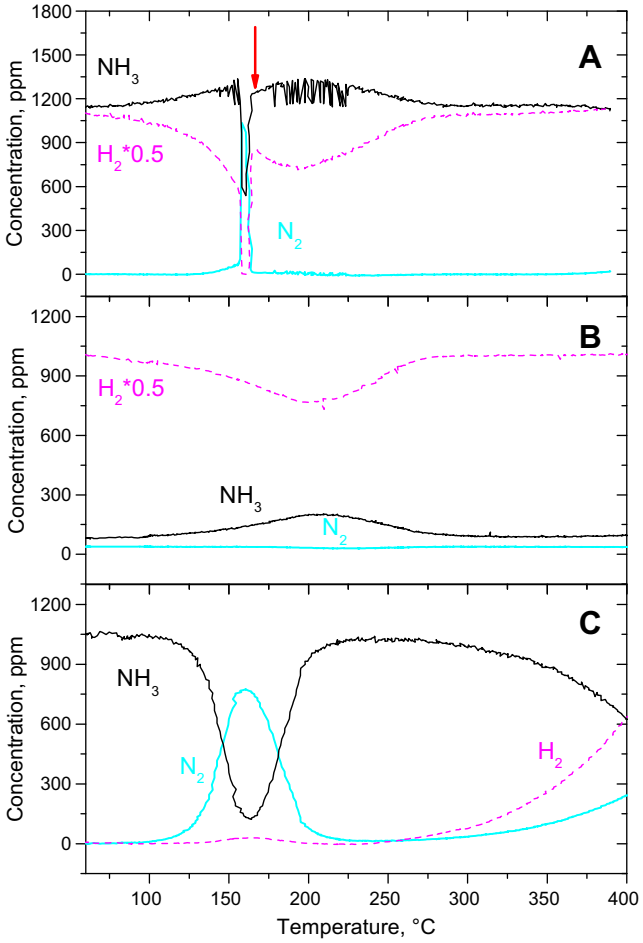

Fig. 9. (A) Competitive $H_2 + NH_3$-TPSR (2000 ppm + 1% v/v H_2O in He) over the Pt—K/Al_2O_3 catalyst after NO/O_2 adsorption at 350 °C; (B) H_2-TPSR (2000 ppm + 1% v/v H_2O in He); and (C) NH_3-TPSR (1000 ppm + 1% v/v H_2O in He) subsequent to a competitive $H_2 + NH_3$-TPSR (2000 ppm + 1% v/v H_2O in He) stopped near 170 °C.

In order to further investigate these aspects, and in particular (i) the presence of adsorbed NO_x species having different reactivity (see the H_2 consumption peak near 200 °C) and (ii) the hydrogen inhibition on ammonia reactivity, additional experiments have been carried out. In particular, H_2/NH_3-TPSR runs have been performed during which the $NH_3 + H_2$ flow has been stopped near 170 °C, after the nitrogen evolution (see the arrow in Fig. 9A). Then the reactor has been cooled at RT in flowing He in order to preserve the NO_x species left unreacted onto the catalyst surface. Subsequent H_2- and NH_3-TPSR runs have been carried out with H_2 and NH_3, respectively, to analyse the reactivity of the residual NO_x adsorbed species. The results are shown in Fig. 9B (H_2-TPSR) and C (NH_3-TPSR).

In the case of the H_2-TPSR run (Fig. 9B), the H_2 concentration shows a minimum near 210 °C, accompanied by NH_3 evolution. Notice that the H_2 consumption is never complete and the minimum corresponds to that observed at the same temperature in the H_2 concentration profiles during both the H_2- and H_2/NH_3-TPSR experiments previously discussed (Figs. 7A and 9A, respectively).

A different picture is apparent in the case of the NH_3-TPSR run (Fig. 9C). Indeed, in this case, NH_3 consumption is observed at low temperatures, starting from 110 °C; ammonia consumption is accompanied by nitrogen evolution only.

Hence, it appears that the treatment with H_2/NH_3 up to 170 °C leaves on the catalyst surface adsorbed NO_x species characterized by poor reactivity towards H_2, and leading to the formation of NH_3 only, as expected. Indeed, as shown above, N_2 formation involves NH_3: however, due the presence of high H_2 concentration, the reactivity of the formed NH_3 in the production of N_2 is inhibited, and accordingly NH_3 is detected unreacted at the reactor outlet. At variance, NH_3 alone results less sensitive to the nature of the adsorbed NO_x species that are always reduced leading to the formation of N_2.

On the basis of these results, if we look backward to dry and wet H_2-TPSR (Figs. 5A and 7A, respectively), the complete NH_3 selectivity which is observed in correspondence of the high-temperature H_2 consumption peak is related to the H_2 inhibition on the NH_3 + nitrate reaction, being in this temperature range the H_2 concentration not null. The important conclusion is that the reduction of the less reactive NO_x species towards H_2 (shoulder at 200–220 °C in the H_2 concentration profile) gives only NH_3 because H_2 is not completely consumed and inhibits ammonia reactivity.

3.7. TPSR of stored NO_x with H_2 or NH_3 in the presence of CO_2 and water

In the previous study over Pt—Ba/Al_2O_3 catalyst [25], it has been found that CO_2 inhibits both the initial reduction of nitrates to

ammonia by H_2 (step 1) and the subsequent reaction of ammonia with the stored nitrates as well (step 2).

To investigate the effect of the co-presence of carbon dioxide and water on the reduction of the stored nitrates over Pt—K/Al_2O_3 catalyst, H_2- and NH_3-TPSR experiments have been performed in the presence of CO_2 (3000 ppm) and H_2O (1% v/v).

In the case of the H_2-TPSR experiment (Fig. 10A), hydrogen is consumed starting from 130 °C and shows an almost complete consumption at 200–210 °C. Then its concentration increases, and a second consumption peak is apparent with minimum of 1300 ppm near 265 °C. The shape of the H_2 concentration trace and the temporal evolution of the reduction products are similar to that described in the case of H_2-TPSR experiment carried out in the absence of CO_2 (Fig. 7A), but are shifted towards higher temperatures. This indicates that also over Pt—K/Al_2O_3 catalyst, the presence of CO_2 inhibits the reaction of the stored nitrates with H_2. This result is confirmed by FT-IR measurements discussed later on.

The results of the NH_3-TPSR run carried out in the presence of water and CO_2 are shown in Fig. 10B. A NH_3 consumption peak is seen starting from near 130 °C, as apparent from N_2 evolution, with a broad minimum centred at 200 °C. A correspondent broad evolution of nitrogen is observed in the range 130–280 °C, which obeys the stoichiometry of reaction (10). At high temperatures, above 300–350 °C, the decomposition of NH_3 to give H_2 and N_2 is observed.

The comparison with the TPSR experiment carried out in the absence of CO_2 (Fig. 7B) shows that also the reduction of the stored NO_x with NH_3 is slightly inhibited in the presence of CO_2, as in the case of H_2. Indeed, the H_2 and NH_3 consumption onset temperatures are shifted towards higher temperature, from 80 °C to 130 °C for H_2, and from 105 °C to 130 °C for NH_3.

The effect of CO_2 on the reduction of the stored NO_x has also been investigated by FT-IR measurements upon admission of H_2 (5 mbar) and CO_2 (10 mbar) at increasing temperature on NO_x stored at 350 °C, and results are shown in Fig. 11A. Note that these experiments have been performed in the absence of water for sake of clarity, being modest the promoting effect of water with respect to inhibiting effect of CO_2.

Upon heating at 100 °C, no sensible changes are observed in the spectra of the stored nitrates (data not reported). Conversely, at 120 °C, the intensity of the bidentate nitrate peaks ($\nu_{N=O}$, $\nu_{O-N-O,asym}$ and $\nu_{O-N-O,sym}$ modes at 1536, 1315 and 1010 cm^{-1}, respectively) starts to decrease (curve b), the decrease being more marked at 150 °C (curve c). Simultaneously, the bands related to ionic nitrates ($\nu_{NO3,asym}$ mode split at 1392 and 1368 cm^{-1} and $\nu_{NO3,sym}$ mode at 1045 cm^{-1}) slightly increase in intensity, due to an increase of the surface hydration related to the reduction process, as observed in the case of H_2 alone (Fig. 9A). However, differently from the case of pure hydrogen, the temperature increase at

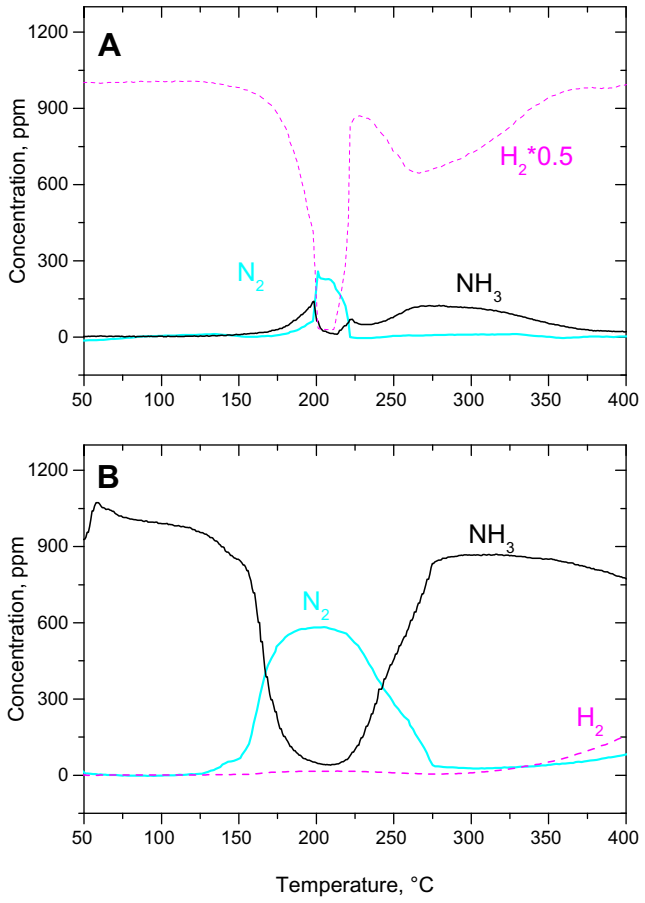

Fig. 10. (A) $H_2/H_2O—CO_2$-TPSR (2000 ppm + 1% v/v H_2O + 0.3% v/v CO_2 in He); (B) $NH_3/H_2O—CO_2$-TPSR (1000 ppm + 1% v/v H_2O + 0.3% v/v CO_2 in He) after NO/O_2 adsorption at 350 °C over the Pt—K/Al_2O_3 catalyst.

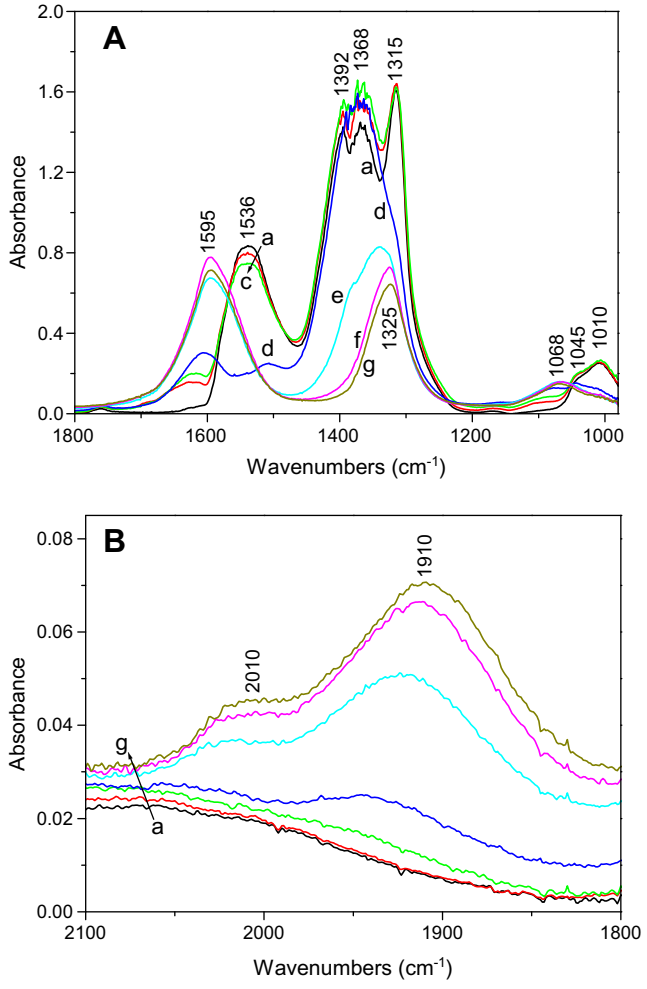

Fig. 11. FT-IR spectra recorded upon admission of H_2 (5 mbar) and CO_2 (10 mbar) mixture at increasing temperature on NO_x stored at 350 °C. (A) Nitrate region, (B) Pt-carbonyl region. Curve a: spectrum of the NO_x stored by NO/O_2 at 350 °C, evacuated at 350 °C and cooled down to 100 °C. Curves b–g, spectra recorded upon admission of H_2/CO_2 mixture at: 120 °C for 10 min (curve b), 150 °C for 10 min (curve c), 200 °C for 10 min (curve d), 250 °C for 10 min (curve e), 300 °C for 10 min (curve f), 350 °C for 10 min (curve g).

200 °C (curve d) does not cause the complete reduction of bidentate nitrates and ionic ones are almost unaffected. At 250 °C, bidentate nitrates are no more observable, but the reduction of ionic nitrates is not yet complete. Contemporary to the consumption of nitrates, chelating bidentate carbonates ($\nu_{C=O}$, $\nu_{O-C-O,asym}$ and $\nu_{O-C-O,sym}$ modes at 1595, 1325 and 1068 cm^{-1}, respectively) are formed on the sites left free by the nitrates. It is necessary to raise the temperature at 300 °C to complete the nitrate reduction, while with pure H_2 the reduction is complete already at 250 °C.

These observations are in agreement with the TPSR measurements previously discussed (Fig. 10A) that pointed out an inhibiting effect of CO_2 on the reduction step. As already proposed in the case of Pt—Ba/Al_2O_3 catalyst [25], the observed inhibiting effects of CO_2 on the reduction steps are related to the poisoning of CO on the Pt sites, CO being formed upon reduction of CO_2 by H_2 according to the Reverse WGSR:

$$CO_2 + H_2 \rightarrow CO + H_2O \quad (12)$$

As a matter of fact, examining the Pt-carbonyl region (Fig. 11B), two bands at 2010 and 1910 cm^{-1} both assignable to CO linear bonded to Pt [30] increase on increasing temperature starting from 150 °C. In particular, the observed frequencies correspond to low Pt coverage by CO. A similar effect was also pointed out by Choi et al. [38].

3.8. Mechanistic aspects of the reduction of the stored nitrates over Pt—K/Al_2O_3

The results obtained from the combined use of transient reactivity experiments and FT-IR spectroscopy point out that nitrates are stored over Pt—K/Al_2O_3 at 350 °C and start to be reduced by H_2 in wet or dry conditions near 100 °C, leading initially to the formation of ammonia (Fig. 7A). Then, the formed ammonia produces N_2 by reaction with the residual stored nitrates. Notably, complete selectivity to nitrogen is observed in the reduction of nitrates with NH_3. These data are consistent with the in series 2-steps molecular pathway already proposed for N_2 formation in the case of Pt—Ba/Al_2O_3 [24–27,35,36] and involving at first the formation of ammonia upon reaction of nitrates with H_2, followed by the reaction of the so-formed ammonia with the residual stored nitrates leading to the selective formation of N_2. The sum of these reactions leads to the overall stoichiometry for the reduction of nitrates by H_2 observed during ISC experiments, i.e. reaction (5) in the case of Pt—K/Al_2O_3 catalyst (Fig. 1).

In the case of the Pt—Ba/Al_2O_3 catalyst sample considered in previous works [24–26], the reduction of the stored nitrates with hydrogen to give ammonia (reaction (7)) has been found to be very fast, being observed slightly above the ambient temperature in the presence of water. On the other hand, the subsequent reaction of ammonia with the residual stored nitrates to give nitrogen is much slower (reaction (8)), and hence has been considered the rate determining in the formation of nitrogen. In line with the suggested two-steps mechanism for N_2 formation, in the case of the Pt—Ba/Al_2O_3 catalyst sample, a significant increase in the N_2 selectivity is observed upon increasing the temperature [24–26]. This is shown in Fig. 12, which reports the N_2 selectivity values obtained during a number of ISC experiments carried out with H_2 as reductant over the Pt—Ba/Al_2O_3 catalyst at various temperatures and under various atmospheres (He, He + H_2O, He + H_2O + CO_2). The N_2 selectivity values are compared with those obtained in the case of the Pt—K/Al_2O_3 catalyst used in this study under the same experimental conditions. From the figure, it clearly appears that in the case of the Pt—Ba/Al_2O_3 catalyst very poor N_2 selectivity is obtained when the regeneration of the trap is carried out at low temperatures. In fact over Pt—Ba/Al_2O_3 at low temperature, H_2 reacts with surface nitrates to give NH_3 (reaction (7)), but ammonia can hardly react with the stored nitrates to form N_2 (reaction (8)).

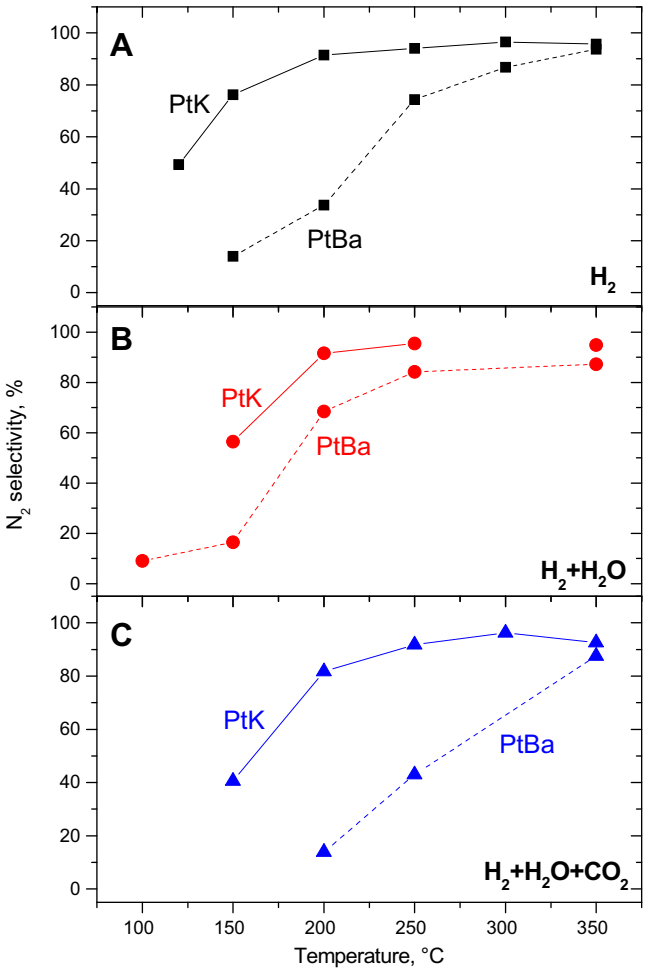

Fig. 12. N_2 selectivity for Pt—K/Al_2O_3 and Pt—Ba/Al_2O_3 catalysts during isothermal reduction performed in (A) H_2 + H_2O, (B) H_2 and (C) H_2 + H_2O + CO_2 at different temperature in the range 100–350 °C.

As a result, ammonia is by far the major reaction product and the nitrogen selectivity is very small. Upon increasing the reduction temperature, the reactivity of NH_3 with nitrates (reaction (8)) becomes appreciable and this drives the selectivity to N_2. Since in the case of the Pt—Ba/Al_2O_3 catalyst sample H_2 is by far more reactive than NH_3 towards surface nitrates, NH_3 reacts only with nitrates located downstream the H_2 front, i.e. when the H_2 concentration is null. Accordingly, N_2 is observed at first at the reactor outlet (Fig. 1D) and the selectivity to NH_3 decreases upon increasing the temperature (Fig. 12).

In the case of the Pt—K/Al_2O_3 sample, the results of H_2- and NH_3-TPSR runs pointed out that the proposed in series two-steps molecular pathway for N_2 formation is operating as well. Like the Pt—Ba/Al_2O_3 sample, the occurrence of a fast reduction step of the adsorbed nitrates by H_2 to give ammonia and the integral "plug-flow" behaviour of the reactor imply the complete consumption of the reductant H_2 and the formation of an H_2 front travelling along the reactor axis [24–26] (Fig. 13). Accordingly, different zones are present in the trap at a given time of the rich phase, i.e. (i) a zone upstream the H_2 front where the trap has already been regenerated; (ii) the zone corresponding to the development of the H_2 front where the formation of ammonia takes place; (iii) a zone immediately downstream the H_2 front where nitrates react with ammonia formed upstream leading to nitrogen formation; and (iv) the last part of the trap with the initial nitrates loading. However, at variance with that observed in the case of the

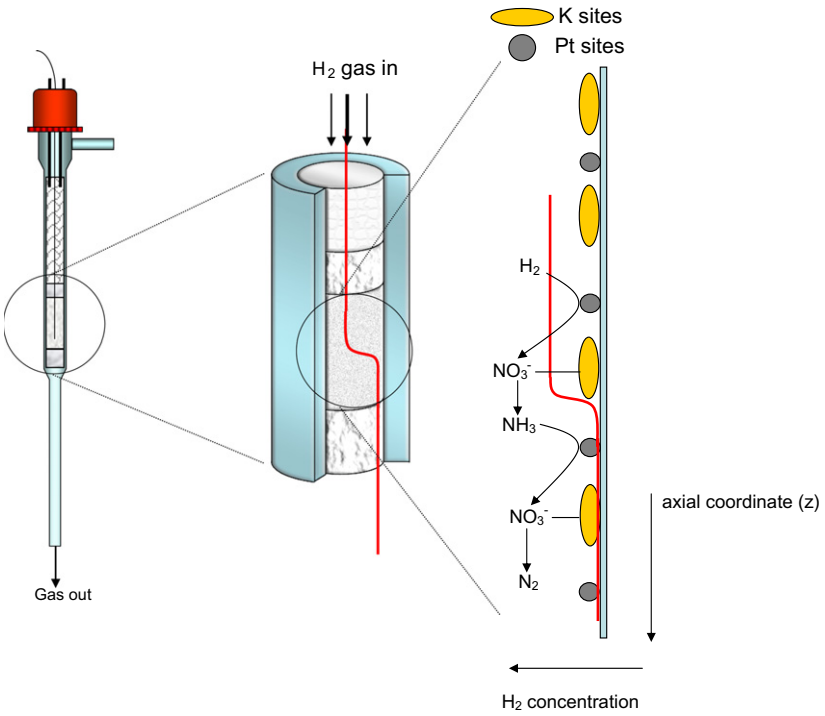

Fig. 13. The "H_2 front" model for the reduction of the stored NO_x.

$Pt—Ba/Al_2O_3$ catalyst sample, the onset for the H_2 + nitrate reaction leading to ammonia (step 1) is observed at higher temperatures if compared to $Pt—Ba/Al_2O_3$ in the presence of water and at lower temperatures in the absence of water (see Figs. 7A and 5A, respectively), whereas the threshold for the NH_3 + nitrate reaction leading to N_2 (step 2) is always seen at lower temperatures (Fig. 7B and 5B, respectively). As a result, the temperature thresholds for steps 1 and 2 are very close for the K-containing catalyst: accordingly ammonia, once formed upon reaction of H_2 with nitrates, readily reacts with residual nitrates leading to the formation of N_2, and this drives the selectivity to N_2 of the reduction process. This explain why the N_2 selectivity obtained in the case of the $Pt—K/Al_2O_3$ catalyst sample is always much higher than that observed over $Pt—Ba/Al_2O_3$ (Fig. 12).

It is worth to note that H_2 shows a strong inhibiting effect towards the reaction of ammonia with nitrates. Hence the reaction between NH_3 and the stored nitrates (leading to N_2 formation) is confined only downstream the H_2 front (see Fig. 13), i.e. when the H_2 concentration is nil. Since an H_2 front is established during the ISC runs (Fig. 1), N_2 is readily and extensively produced in these runs; on the other hand, a higher NH_3 formation is observed during TPSR experiments since complete H_2 consumption is observed only in a narrow temperature range.

Detailed mechanistic aspects of the reduction of adsorbed nitrates with H_2 and with NH_3 are not yet understood. Being the reaction catalysed by Pt, it is speculated that H_2 is activated over the Pt sites, and spills-over towards the stored nitrates which are reduced to ammonia. How nitrates are reduced by H adspecies and the role of Pt in this reaction are still under discussion, along with mechanistic details for the Pt-catalysed reaction between NH_3 and nitrates leading to N_2. Moreover, the diffusion of nitrates towards reduced Pt sites, as discussed above, cannot be excluded. However the observation that during the initial part of the TPSR experiments H_2 and NH_3 are consumed with no evolution of gaseous species suggests the involvement of short-lively reduced intermediate surface species, e.g. nitrites, undetected by FT-IR spectroscopy being very reactive in the further reduction to NH_3 or N_2. As a matter of fact, nitrite intermediate surface species have been pointed out upon reduction of the stored nitrates by CO over the same $Pt—Ba/Al_2O_3$ catalyst [39]. Being CO less effective than H_2 in the reduction of the stored nitrates, this allowed the detection of surface intermediates. Notably, the features observed after interaction of ammonia at RT with the catalyst surface suggest the adsorption of NH_3 on the K^+ ions (i.e. K^+O^{2-} pairs with strongly basic O^{2-}). It is suggested that this activated ammonia species reacts with the suggested nitrite species (or with N-adspecies having nitrogen oxidation state +3, like nitrosonium ions, NO^+) giving rise to an ammonium nitrite or nitrosamide intermediate, respectively, that then decomposes to nitrogen and water, in line with the chemistry proposed in the case of NH_3-SCR reaction [40,41].

The different reactivity of $Pt—K/Al_2O_3$ and $Pt—Ba/Al_2O_3$ towards the activation of both hydrogen and ammonia in the reduction of the stored NO_x could be related either to a different reactivity of the adsorbed NO_x species or to a change in the activity of the Pt active sites in the reduction process due to the presence of the different storage component (K vs. Ba), or both. A comparison of the features of the NO_x species adsorbed over $Pt—Ba/Al_2O_3$ [8,11] with those stored on $Pt—K/Al_2O_3$ points out significant differences between the NO_x species stored on the two investigated catalytic systems. Along similar lines, recent FT-IR characterization studies [11,42] point out that the Pt active sites are modified by the presence of K or Ba due to the strong electronic interaction between the alkaline/alkaline-earth oxide and the noble metal. Spectroscopic studies performed in our laboratories by using CO as adsorbate to probe the state of the Pt sites, pointed out a strong interaction of Pt with the basic K sites. Indeed, the presence of three bands markedly red-shifted with respect to carbonyl bands seen on Pt/Al_2O_3 (from 2060 cm^{-1} to 2015 cm^{-1} due to linear carbonyls on Pt^0, from 1845 cm^{-1} to 1745 cm^{-1} due to bridged CO) has been observed. The influence of the K phase, that enhances the electron density on Pt, favours the formation of bridged carbonyls towards linear ones, as reported in the literature [30,31]. Worth to note that

the interaction between Pt and Ba sites results in a band due to linear Pt carbonyls that is shifted to lower frequencies with respect to carbonyl bands seen on Pt/Al_2O_3 (from 2090 to 2046 cm^{-1}) [31], but this red-shift is lower than in the case of K-system. Also in this case, the appearance of bands assigned to multi-bridged CO species (band near 1750 cm^{-1}) could be a further indication of Pt atoms strongly interacting with the barium phase, probably with partial negative charge. These FT-IR evidences together with the shifts observed in the band positions seems to indicate that K has a stronger electronic effect over Pt sites than Ba.

Accordingly, it is likely that the different reactivity between $Pt—K/Al_2O_3$ and $Pt—Ba/Al_2O_3$ towards H_2 and NH_3 is explained, at least partially, by the electronic state of Pt. It is indeed well known that the activation of hydrogen goes through a dissociative adsorption on Pt sites by weakening the H—H bond and forming a Pt—H bond. The competition between H_2 and NH_3 for the activation on Pt sites also suggests that the activation of ammonia goes through the formation of a Pt—H bond by weakening the N—H bond. Hence, the higher electron density on Pt in the case of K-containing catalyst than on Ba-containing sample may govern the reactivity of the catalysts towards H_2 and NH_3, although the different nature of the NO_x stored species present on these catalysts may play a role as well.

4. Conclusive remarks

In the present paper, the nature of stored NO_x and mechanistic aspects of the reduction of NO_x stored over a model $Pt—K/Al_2O_3$ catalyst sample has been investigated by combined transient reactivity studies and FT-IR spectroscopy. A comparison with a model $Pt—Ba/Al_2O_3$ catalyst has also been made.

It has been found that at 350 °C on both the K- and Ba-containing catalysts, the storage proceeds with formation of nitrites at the beginning of the storage. In particular on $Pt—K/Al_2O_3$ catalyst both chelating and linear nitrites are observed, differently from the case of $Pt—Ba/Al_2O_3$ where only chelating nitrites were observed. Nitrites are then oxidized to nitrates; a parallel pathway involving the direct formation of nitrates species (dismutation process from NO_2) is also apparent. At saturation, only nitrates are present on the catalyst surface over both $Pt—K/Al_2O_3$ and $Pt—Ba/Al_2O_3$; however, whereas bidentate nitrates are present in remarkable amounts on $Pt—K/Al_2O_3$, along with ionic nitrates, only very small amounts of bidentate nitrates were observed on $Pt—Ba/Al_2O_3$.

The reduction of the stored NO_x has been studied with H_2 as reductant. The study has pointed out that under nearly isothermal conditions N_2 formation occurs via an in series two-steps Pt-catalysed molecular process involving the formation of ammonia as an intermediate. The first step of the series is ammonia formation through the reaction of H_2 with stored nitrates; ammonia then reacts with the nitrates left on the catalyst surface leading to the formation of nitrogen. This scheme is very similar to that already proposed in the case of the $Pt—Ba/Al_2O_3$ catalyst sample, but in the case of the K-containing catalyst lower amounts of NH_3 have been detected at the reactor outlet, being N_2 by far the most abundant product. As pointed out by dedicated experiments carried out with NH_3 as reactant, the higher N_2 selectivity observed in the case of the $Pt—K/Al_2O_3$ catalyst is due to the fact that the onset for the H_2 + nitrate reaction leading to ammonia (step 1) occurs at temperatures very close to the threshold for the NH_3 + nitrate reaction leading to N_2 (step 2). Accordingly, ammonia, once formed, readily reacts with surface nitrates to give N_2, and this drives the selectivity of the reduction process to N_2.

Notably, over $Pt—K/Al_2O_3$, a strong inhibition of H_2 on the reactivity of NH_3 towards nitrates has been pointed out, likely due to a competition of H_2 and NH_3 for the activation at the noble metal sites. In fact, only when the H_2 concentration is null ammonia reacts with nitrates and N_2 formation is apparent. The H_2 inhibition on the N_2 formation via step 2 does not imply a low N_2 selectivity during the isothermal reduction of nitrates since NH_3 reacts with NO_x stored downstream the H_2 front, where the H_2 concentration is null. Notably, the competition of H_2 and NH_3 on the activation on the Pt sites is not clearly apparent in the case of the $Pt—Ba/Al_2O_3$ sample due to the very large difference in the temperature thresholds for the reaction of H_2 and NH_3 with the stored nitrates.

Finally, the effects of water and CO_2 on the reduction process are also addressed. Water showed a slight promoter effect on the onset temperature of H_2 consumption and no effect on the subsequent reaction of ammonia with stored nitrates, whereas CO_2 has a strong inhibition effect on both the reduction of nitrates by H_2 and ammonia, due to poisoning of Pt by CO formed upon CO_2 hydrogenation.

References

[1] N. Takahashi, H. Shinjoh, T. Iijima, T. Suzuki, K. Yamazaki, K. Yokota, H. Suzuki, N. Miyoshi, S. Matsumoto, T. Tanizawa, T. Tanaka, S. Tateishi, K. Kasahara, Catal. Today 27 (1996) 63.
[2] W. Epling, L. Campbell, A. Yezerets, N. Currier, J. Parks, Catal. Rev. Sci. Eng. 46 (2004) 163.
[3] N. Miyoshi, S. Matsumoto, K. Katoh, T. Tanaka, J. Harada, N. Takahashi, K. Yokota, M. Sugiura, K. Kasahara, SAE Technical Paper 950809, 1995.
[4] T. Johnson, Platinum Metals Rev. 52 (2008) 23.
[5] M. Takeuchi, S.I. Matsumoto, Top. Catal. 28 (2004) 151.
[6] M. Konsolakis, I.V. Yentekakis, Appl. Catal. B 29 (2001) 103.
[7] H. Mahzoul, J.F. Brilhac, P. Gilot, Appl. Catal. B 20 (1999) 47.
[8] F. Prinetto, G. Ghiotti, I. Nova, L. Lietti, E. Tronconi, P. Forzatti, J. Phys. Chem. B 105 (2001) 12732.
[9] E. Fridell, M. Skoglundh, B. Westerberg, S. Johanson, G. Smedler, J. Catal. 183 (1999) 196.
[10] L. Lietti, P. Forzatti, I. Nova, E. Tronconi, J. Catal. 204 (2001) 175.
[11] I. Nova, L. Castoldi, F. Prinetto, G. Ghiotti, L. Lietti, E. Tronconi, P. Forzatti, J. Catal. 222 (2004) 377.
[12] M. Piacentini, M. Maciejewski, A. Baiker, Appl. Catal. B 66 (2006) 126.
[13] A. Scotti, I. Nova, E. Tronconi, L. Castoldi, L. Lietti, P. Forzatti, Ind. Eng. Chem. Res. 43 (2004) 4522.
[14] T.J. Toops, D.B. Smith, W.P. Partridge, Appl. Catal. B 58 (2005) 245.
[15] T.J. Toops, D.B. Smith, W.S. Epling, J.E. Parks, W.P. Partridge, Appl. Catal. B 58 (2005) 255.
[16] T.J. Toops, D.B. Smith, W.P. Partridge, Catal. Today 114 (2006) 112.
[17] T. Lesage, J. Saussey, S. Malo, M. Hervieu, C. Hedouin, G. Blanchard, M. Daturi, Appl. Catal. B 72 (2007) 166.
[18] I. Nova, L. Castoldi, L. Lietti, E. Tronconi, P. Forzatti, F. Prinetto, G. Ghiotti, SAE Technical Paper 2005-01-1085.
[19] R. Burch, J. Breen, F. Meunier, Appl. Catal. B 39 (2002) 283.
[20] I. Nova, L. Castoldi, L. Lietti, E. Tronconi, P. Forzatti, SAE Technical Paper 2006-01-1368.
[21] L. Castoldi, I. Nova, L. Lietti, P. Forzatti, Catal. Today 96 (2004) 43–52.
[22] L. Castoldi, I. Nova, L. Lietti, E. Tronconi, P. Forzatti, Top. Catal. 42–43 (2007) 189.
[23] I. Nova, L. Lietti, L. Castoldi, E. Tronconi, P. Forzatti, J. Catal. 239 (2006) 244–254.
[24] I. Nova, L. Lietti, P. Forzatti, Catal. Today 136 (2008) 128.
[25] L. Lietti, I. Nova, P. Forzatti, J. Catal. 257 (2008) 270.
[26] P. Forzatti, L. Lietti, I. Nova, Energy Environ. Sci. 1 (2008) 236.
[27] S.S. Mulla, S.S. Chaugule, A. Yezerets, N.W. Currier, W.N. Delgass, F.H. Ribeiro, Catal. Today 136 (2008) 136.
[28] N. Miyoshi, T. Tanizawa, K. Kasahara, S. Tateishi, European Patent Application 0 669 157 A1, 1995.
[29] I. Nova, L. Castoldi, F. Prinetto, V. DalSanto, L. Lietti, E. Tronconi, P. Forzatti, G. Ghiotti, R. Psaro, S. Recchia, Top. Catal. 30/31 (2004) 181.
[30] F. Prinetto, M. Manzoli, S. Morandi, F. Frola, G. Ghiotti, L. Castoldi, L. Lietti, P. Forzatti, J. Phys. Chem. C 114 (2010) 1127.
[31] F. Frola, M. Manzoli, F. Prinetto, G. Ghiotti, L. Castoldi, L. Lietti, J. Phys. Chem C 112 (2008) 12869.
[32] F. Prinetto, G. Ghiotti, I. Nova, L. Castoldi, L. Lietti, F. Tronconi, P. Forzatti, Phys. Chem. Chem. Phys. 5 (2003) 4428.
[33] Unpublished results (Paschetta E. "Caratterizzazione chimico-Fisica di catalizzatori per l'abbattimento di ossidi d'azoto prodotti da veicoli a combustione magra". Tesi di Laurea Magistrale- Università di Torino. Luglio 2008).
[34] L. Cumaranatunge, S.S. Mulla, A. Yezerets, N.W. Currier, W.N. Delgass, F.H. Ribeiro, J. Catal. 246 (2007) 29.
[35] P. Forzatti, L. Lietti, N. Gabrielli, Appl. Catal. B 99 (2010) 145.
[36] D. Bhatia, R.D. Clayton, M.P. Harold, V. Balakotaiah, Catal. Today 147 (2009) S250.

[37] J.-Y. Luo, W.S. Epling, Appl. Catal. B 97 (2010) 236.
[38] J.–S. Choi, W.P. Partridge, C.S. Daw, Appl. Catal. A 293 (2005) 24.
[39] P. Forzatti, L. Lietti, I. Nova, S. Morandi, F. Prinetto, G. Ghiotti, J. Catal. 274 (2010) 163.
[40] G. Busca, L. Lietti, G. Ramis, F. Berti, Appl. Catal. B 18 (1998) 1.
[41] G. Ramis, G. Busca, F. Bregani, P. Forzatti, Appl. Catal. 64 (1990) 259.
[42] G. Fornasari, F. Trifirò, A. Vaccari, F. Prinetto, G. Ghiotti, G. Centi, Catal. Today 75 (2002) 421.